



CENTRO INTERNACIONAL DE ESTUDOS
DE DOUTORAMENTO E AVANZADOS
DA USC (CIEDUS)

TESE DE DOUTORAMENTO

**THEORETICAL AND
COMPUTATIONAL
STUDY OF MIXTURES OF
IONIC LIQUIDS WITH
ADDITIVES OF
TECHNOLOGICAL INTEREST IN
THE PRESENCE OF
INTERFACES**

Víctor Gómez González

ESCOLA DE DOUTORAMENTO INTERNACIONAL
PROGRAMA DE DOUTORAMENTO EN CIENCIA DE MATERIAIS

SANTIAGO DE COMPOSTELA

2018





DECLARACIÓN DO AUTOR/A DA TESE

Theoretical and computational study of mixtures of ionic liquids with additives of technological interest in the presence of interfaces

D. Víctor Gómez González

Presento a miña tese, seguindo o procedemento axeitado ao Regulamento, e declaro que:

- 1) A tese abarca os resultados da elaboración do meu traballo.
- 2) De selo caso, na tese faise referencia ás colaboracións que tivo este traballo.
- 3) A tese é a versión definitiva presentada para a súa defensa e coincide coa versión enviada en formato electrónico.
- 4) Confirmo que a tese non incorre en ningún tipo de plaxio doutros autores nin de traballos presentados por min para a obtención doutros títulos.

En Santiago de Compostela, a 15 de Xullo de 2018

Asdo: Víctor Gómez González.







AUTORIZACIÓN DO DIRECTOR / TITOR DA TESE

Theoretical and computational study of mixtures of ionic liquids with additives of technological interest in the presence of interfaces

D. Luis Javier Gallego del Hoyo e D. Luis Miguel Varela Cabo, catedráticos da área de Física da Materia Condensada, do Departamento de Física de Partículas da Universidade de Santiago de Compostela,

INFORMAN:

Que a presente tese, correspóndese co traballo realizado por D. Víctor Gómez González, baixo a nosa dirección, e autorizamos a súa presentación, considerando que reúne os requisitos esixidos no Regulamento de Estudos de Doutoramento da USC, e que como directores desta non incorre nas causas de abstención establecidas na Lei 40/2015.

De acordo co artigo 41 do Regulamento de Estudos de Doutoramento, declaramos tamén que a presente tese de doutoramento é idónea para ser defendida en base á modalidade de COMPENDIO DE PUBLICACIÓNS, nos que a participación do/a doutorando/a foi decisiva para a súa elaboración.

A utilización destes artigos nesta memoria, está en coñecemento dos coautores, tanto doutores como non doutores. Ademais, estes últimos teñen coñecemento de que ningún dos traballos aquí reunidos poderá ser presentado en ningunha outra tese de doutoramento.

En Santiago de Compostela, a 15 de Xullo de 2018

Asdo: D. Luis Javier Gallego del Hoyo

D. Luis Miguel Varela Cabo



Summary

Ionic liquids (ILs) are novel materials that have been receiving a lot of attention in the past twenty years, mainly due to the high number of present and future potential technological applications in several fields, but also for their unique role among charged complex fluids. Due to charge and size asymmetries and because they are formed by organic cations and/or anions, they are amphiphilically nanostructured molten salts at room temperature (melting temperature below 100°C). Their areas of application include electrochemistry, thermal storage, lubricants, catalysis and separation, among others. However, their peculiar general properties (low vapor pressure, high thermal stability, high electrical and thermal conductivity and amphiphilicity) allow their consideration as the “green solvents of the future”. Moreover, the great amount of combinations that can be chosen to form an IL with currently known cations and anions provides an enormous flexibility to these compounds, as one could, in principle, tune their properties at will for each specific applications. For this reason, they are currently considered to be “designer solvents”. However, no systematic theory that relates the composition of ILs with their properties has been reached yet, and is one of the major challenges in current chemical physics.

Specifically, in this thesis we deal mainly with electrochemical applications of ILs. The wide electrochemical windows of these ionic materials makes them very attractive candidates to become the next generation of electrolytes in electrochemical devices such as batteries, supercapacitors or fuel cells, where reaching high energy and power densities is crucial. The application of these compounds to batteries, however, usually demands the addition of some redox electroactive species to the solvent, generally an inorganic salt, precisely because of

the wide voltage range over which the liquid is electrochemically inert. Therefore, a proper understanding of ion solvation and transport in the densely ionic environment of an IL is needed in order to rationally develop novel electrolytes, which could be formed by an IL doped with an inorganic salt. In particular, salts of high valence such as those containing Mg and Al are being investigated because they might lead to more efficient energy-storage systems, besides being also more abundant and, consequently, cheaper than those based in lithium (Li), the preferred option for batteries nowadays. The importance of some other salts containing high valence elements, such as Zn or Cr, is also relevant for electrolytic applications. In this context, the microstructure of ILs and, to a greater extent, of their mixtures with salts of electrochemical interest, is of special relevance. Specifically, most of the particular features of ion solvation in ILs are still largely unknown.

One of the most efficient techniques for probing microscopic properties of complex molecular systems and for predicting macroscopic ones is computer simulation. In particular, and given the high number of ILs than can be theoretically produced, these methods can help researchers save both time and money, as the costs of virtually experimenting with ILs are generally much lower than those of performing experiments in real life. Of course, the employed computational method has to be chosen carefully in order to provide reliable results that match the experimental ones, if they are available. Luckily, in the last decades technological advances and research efforts have led to the improvement and development of powerful computational tools, which have been extensively used to study ILs. Despite the undoubted interest for the precise features of ionic coordination in ILs, and despite having been used extensively to analyze bulk and interfacial properties of mixtures with monovalent ions, there have been comparatively few reports of MD simulations of solutions of salts with high valence cations.

In the present thesis, a computational study of mixtures of ILs

with salts of diverse valence was performed, both in bulk conditions and at the electrochemical interface. Our main goal was to analyze the solvation mechanism of salt cations of high valence in ILs, paying special attention to the influence of the salt cation valence in the structure of the mixture and in the complexes that form, as well as in the protic or aprotic character of the IL. Moreover, the charge transfer from the salt cation to an electrode in IL environment was studied. In this thesis, MD simulations were mainly carried out using the open source and free software GROMACS and the standard MD all-atom force field OPLS-AA. Although the force field employed hereby is non-polarizable (polarizable force fields are currently under study), it is known to provide very accurate structural predictions and qualitatively correct trends for transport properties. Moreover, density functional theory (DFT) simulations are also performed to describe metal complexes and charge transfer at the electrochemical interface. In this latter case, three DFT software packages were used: VASP, NWChem and Gaussian. The first one uses plane waves as basis sets, and we choose Perdew-Burke-Ernzerhof (PBE) functional to perform the calculations. The other two use LCAO basis sets (in our case, 6-31G* or 6-311G**), and we employed Becke's three-parameter hybrid functional with gradient-corrected correlation as per Lee, Yang and Parr (B3LYP).

Aiming at gaining insight of the solvation of divalent cations in these densely ionic environments, in Chapter 2.1 we present a detailed analysis of the solvation (structure and single particle dynamics) of divalent cations of Mg^{2+} and Ca^{2+} in mixtures of salts of these metals with an aprotic IL (AIL) and a protic IL (PIL) with a common anion: 1-butyl-3-methylimidazolium hexafluorophosphate ($[\text{BMIM}][\text{PF}_6]$) and ethylammonium nitrate (EAN), respectively. Moreover, in order to test the accuracy of the force field employed in the simulations, experimental measurements of the density of these mixtures were performed in all cases. Their structure was analyzed by means of the density, volumetric properties, radial distribution functions, coordination numbers, and, for PILs, evolution of the hydrogen bonding

network with salt concentration. We also considered, for analyzing single particle dynamics of different species in the mixtures, the velocity autocorrelation function and the vibrational densities of states (vDOS) of the cations of the dissolved salt. Our main goal was to shed light on the coordination mechanisms of divalent cations in bulk ILs and to understand their differences, if any, with monovalent cations. The comparison with experimental values of both densities and apparent molar volumes, V_ϕ , gives a very good agreement, confirming that our employed force field is reliable for these mixtures.^a The constancy of V_ϕ and the fact that its value is close to that of the crystalline salt throughout all salt concentrations suggest that the local environment of the divalent cations remains approximately constant upon addition of salt and similar to that of the solid state of the salt. Radial distribution functions show two coordination modes (monodentate and bidentate) for the salt cation solvation by IL anions, although in the mixture of the PIL with Mg^{2+} the bidentate mode is suppressed. Both facts are consistent with salt cations being solvated in the polar nanoregions of the pure IL, whose structure is not appreciably affected by the addition of salt (as reflected by the constancy of the vDOS of the system upon salt doping), forming a quasi-lattice structure in the polar nanoregions reminiscent of the crystalline salt. On the other hand, the vDOS of salt cations in the mixtures reveals that there are three vibrational modes in mixtures with the studied AIL, while in mixtures with nitrate-based PIL only one is possible, showing different types of coordination in both environments. Moreover, no appreciable shift of the peaks associated to vibrational motions of salt cations in their molecular cages with salt concentration is observed, a behaviour opposite to that of ions in aqueous solution. This provides further evidence that the increase of salt concentration scarcely modifies the environment of the divalent ions. Thus, the main features of the nanostructured solvation of divalent cations in ILs are qualitatively similar to those in the equivalent mixtures with monovalent salts, except for the relatively stronger electrostatic coupling in the polar nanoregions of the mixtures with cations of higher valence, which results in the

^aThe same force field is used in all MD simulations in this thesis.

formation of octahedral instead of tetrahedral solvation complexes when the salt cation is divalent.

Once the structure of mixtures of ILs and divalent salts has been studied, a proper characterization of their behaviour at the electrochemical interface was our following goal. So, in Chapter 2.2 we include a MD study of mixtures of the AIL 1-butyl-3-methylimidazolium tetrafluoroborate ([BMIM][BF₄]) with magnesium tetrafluoroborate (Mg(BF₄)₂) confined between two parallel graphene walls, the first reported one, to the best of our knowledge. The structure of the system was analyzed by means of ionic density profiles, lateral structure of the first layer close to the graphene surface and angular orientations of imidazolium cations. Free energy profiles for divalent magnesium cations were calculated using two different methods in order to evaluate the height of the potential barriers near the walls, and the results were compared to those of mixtures of the same IL and a lithium salt (Li(BF₄)). Preferential adsorption of magnesium cations was analyzed using a simple model and compared to that of mixtures including lithium cations. Besides, the vDOS of Mg²⁺ cations were calculated for the cations close to the walls, analyzing the influence of the graphene surface charge. We confirm that even uncharged graphene walls have an important effect on the structure of the liquid, giving rise to an inhomogeneous charge distribution with oscillating profiles, the so called electric double layer, which extends up to ~ 2 nm of the wall, where homogeneous bulk distributions are recovered. On the other hand, when the wall is charged, a strong layering of charge is produced. This layering of charge, joined to the strong solvation of salt cations by IL anions, cause salt cations to be closer to the positively charged wall than to the negatively charged one. Lateral structure of the mixtures near the walls shows that, as has been previously reported for IL-water mixtures, transitions from time-averaged stripes to ordered phases with hexagonal symmetry take place upon doping of the IL. Moreover, a herringbone interfacial 3D structure appears, implying that the first layers of the electric double layer are strongly coupled by Coulomb interactions, which is

further reinforced by salt cations introduced in the system. At neutral walls, the most probable configuration for imidazolium cation rings is to lie almost parallel to the wall, independently of the concentration of added salt, although charging the wall changes neatly the distribution of orientations. Analyzing the free energy profiles for salt cations near the wall, divalent cations are seen to face higher barriers than monovalent ones as they approach the electrode, a fact that is also reflected in the calculations of the preferential adsorption of both salt cations. vDOS of the salt cations reveal a red shift of the peaks relative to those of bulk mixtures, which means that salt cations are less strongly bound in their cages in the interfacial region than they are in the bulk, an opposite behaviour to that of water molecules in ILs. The main conclusion is that divalent cations more hardly reach the electrochemical interface than their monovalent counterparts, due to the higher potential barriers they face caused by the very stable solvation complexes formed by these metal cations.

Up to now, AILs, which are known to form weak hydrogen bonds, have dominated the electrochemical applications at the expense of those that form stronger hydrogen bonds (PILs), although in the last few years the usage of the latter seems to have gained more interest. However, despite the crucial importance of hydrogen bonding in the microstructure of ILs and their mixtures, up to our knowledge, no computational studies of PILs mixed with 1:1 or 2:1 salts at the electrochemical interface have been previously reported. The work in Chapter 2.3 tries to fill that gap by performing MD simulations of mixtures of ethylammonium nitrate (EAN) with lithium and magnesium nitrates confined between two parallel graphene walls (both in the neutral and charged states). In order to analyze the influence of the salt cation charge, that of hydrogen bonds (using a PIL that forms strong hydrogen bonds), and the charge of the interface on the structure of the electric double layer at the electrochemical interface, we computed molecular density profiles, angular orientations of IL cations and the lateral structure of the innermost layer of the electric double layer close to the graphene wall. We also performed a

dynamical analysis calculating the vDOS of the salt cations near the graphene walls and compared them to those in the bulk. Finally, we investigated the structure of the system containing lithium nitrate at the interface using *ab initio* DFT calculations. Angular orientation of IL cations reveals that the main difference with the non hydrogen bonded aprotic mixtures is the preference of the cations in the latter to lie flat to the wall in the neutral case, because of the different symmetry of the cation, and the existence of a wider range of orientations in the charged situations. Analysis of the lateral structure of the mixture of salt and the PIL shows that hydrogen bonds lead to more marked polar and apolar zones. Comparing the vDOS for the monovalent and divalent cations near the walls, a red shift of the peak associated to the only vibrational mode relative to that in bulk mixtures with lithium appears, but this displacement is absent in the case of mixtures with magnesium. All these results allow to conclude that salt cations in protic environments are able to reach more easily the negatively charged wall than the same cations in the studied AIL, although within the same kind of IL, a higher valence of the metal cation means stronger binding in solvation complexes and, hence, more difficulties for reaching the electrochemical walls. Our detailed DFT results suggest that the differences between DFT-calculated salt cation charges near the wall and the classical MD charges might be important regarding the behaviour of the system, and therefore a more precise study of the charge transfer would be necessary.

On the other hand, despite the growing interest in the potential electrochemical applications of both aluminium and ILs in batteries, the microstructure of mixtures of trivalent salts with these densely ionic solvents is completely unknown. In this work (Chapter 2.4), we complete the study of ILs doped with electrochemical salts analyzing the solvation of an aluminium salt in a PIL with common anion. For this purpose, MD simulations of mixtures of a PIL, EAN, with aluminium nitrate ($\text{Al}(\text{NO}_3)_3$), both in bulk and confined between graphene walls, were performed. Several structural quantities of the system were calculated for different salt concentrations, such as

densities, radial distribution functions, structure factors, coordination numbers and hydrogen bonds for the bulk mixture, and ionic density profiles for the confined ones. Moreover, vDOS for the salt cations, both in bulk and close to the walls, are calculated. The results obtained were analyzed and compared to those for mixtures of EAN with monovalent and divalent salts, in order to probe the influence of the salt cation charge on the system's properties. Finally, *ab initio* DFT calculations were performed in order to analyze the structure of the Al^{3+} -ligand complexes, and their predictions for the Raman spectra were compared both to the corresponding experimental one and the one coming from MD simulations. The experimental densities and Raman spectra are in good agreement with simulated results, confirming that the parametrization of our trivalent salt cation is reliable. We also find that the electrostatic field of the ion has a great effect in the type of coordination of salt solvation complexes: when it increases, the bidentate coordination mode is progressively attenuated, so in the case of aluminium salt cations only a monodentate coordination mode in the anion complexes is possible. The total structure factor of the mixtures shows the compression of the polar regions of the mixture due to the stronger electrostatic attractive interactions that appear when the added salt is placed there (electrostriction), and that the addition of aluminium salt in the system promotes the short-range order (reflected in the formation of stable solid-like structures and complexes in the polar nanoregions of the liquid) of the system at the expense of long-range order. However, this structural effect does not seem to be substantial. Both coordination numbers and DFT calculations reflect the formation of octahedral salt cation-anion coordination complexes, similarly as in magnesium-based mixtures. Moreover, a detailed analysis of the number of hydrogen bonds per molecule as a function of salt concentration shows again the strong resiliency of the structure of the IL polar regions to the addition of salts of different types. In confined mixtures, the most relevant result is the similarity between divalent and trivalent salts, which approximately reach the same distance to the wall, that is, anyhow, larger than that of monovalent cations in the same PIL. Thus, we conclude in this work that

the structure of mixtures of ILs with aluminium salts is generally very similar to the structure of the mixtures with divalent salts, an effect which might be caused by the existence of IL polar nanoregions which easily accommodate the added salt forming the corresponding solvation complexes (e.g. octahedral aluminium- NO_3^- complexes in EAN- $\text{Al}(\text{NO}_3)_3$ mixtures).

Another essential aspect regarding the electrochemical applications of these densely ionic electrolytes is the electronic charge transfer from the electroactive species to electrodes. Although MD simulations (combined with classical Marcus theory) provide a valuable average picture of this charge transfer, a proper microscopic analysis requires a detailed description of the electronic densities of the reacting species throughout the process, so quantum chemical methods are needed. Following the results from Chapter 2.3, in Chapter 2.5 we used, for the first time, DFT to analyze the charge transfer between lithium or magnesium cations and a graphene wall in three different situations: in vacuum, amongst fluorine atoms to simulate a molten salt, and in an IL. Charges of all the species in the system were analyzed as a function of the distance of the salt atom to the wall in each situation. In the systems which only contain fluorine atoms, these remain ionized almost independently of the salt cation position, and the salt charge is mainly transferred to the wall until the salt atom reaches the distance where the fluorine atoms are placed, where it bonds with them and no further charge transfer to the wall is detected. Finally, the presence of an IL seems to lead to a significant difference in charge transfer, which starts at longer distances than in the other environments, but ultimately leads to the same degree of charge transfer to the electrode. Higher efficiency in the charge transfer process and higher vertical ionization potentials are found for the configuration with the metal closer to the electrode, and the opposite trend is found for the vertical electron affinities, confirming that electronic exchange in the nanoconfined region close to the electrode is energetically favorable. Finally, no relevant difference between monovalent and divalent salt cations is found regarding the charge transfer. Thus, all our results

suggest a certain catalysing effect of ILs as regards metal/electrode charge transfer in these densely ionic environments.

Finally, this thesis ends with a brief summary of the main conclusions and future trends, as well as with a list of its related publications.



Resumen

Los líquidos iónicos (LIs) son novedosos materiales que han comenzado a recibir mucha atención en los últimos veinte años, principalmente debido a su gran número de presentes y futuras aplicaciones tecnológicas en diversos campos, pero también por su rol único dentro de los fluidos cargados complejos. Debido a sus asimetrías de carga y tamaño, además de a estar formados por cationes orgánicos y/o inorgánicos, se consideran sales fundidas a temperatura ambiente anfifílicamente nanoestructuradas (temperatura de fusión por debajo de 100°C). Sus áreas de aplicación incluyen electroquímica, almacenamiento térmico, lubricantes, catálisis y separación, entre otras. Además, sus propiedades generales tan peculiares (baja presión de vapor, alta estabilidad térmica, altas conductividades eléctricas y térmicas y anfifilicidad) hacen que sean considerados como los “disolventes verdes del futuro”. La gran cantidad de combinaciones que pueden ser elegidas para formar un LI con los cationes y aniones actualmente conocidos provee de una enorme flexibilidad a estos compuestos, puesto que uno podría, en principio, cambiar sus propiedades a voluntad para cada aplicación específica. Por esta razón, actualmente son considerados “disolventes de diseño”. Sin embargo, ninguna teoría sistemática que relacione la composición de los LIs con sus propiedades ha sido alcanzada todavía, y este es precisamente uno de los mayores retos en la química física actual.

En concreto, en esta tesis nos centramos principalmente en las aplicaciones electroquímicas de los LIs. La gran ventana electroquímica de estos materiales iónicos los hace unos candidatos muy atractivos para convertirse en la siguiente generación de electrolitos en dispositivos electroquímicos como baterías, supercondensadores o celdas de combustible, donde alcanzar una alta densidad de energía y de

potencia es vital. La aplicación de estos compuestos a baterías, sin embargo, exige normalmente la adición de una especie electroactiva redox, generalmente una sal inorgánica, precisamente por el amplio rango de voltajes en los que el líquido es electroquímicamente inerte. Es necesario, por tanto, un profundo conocimiento de la solvatación y el transporte de los iones en el medio iónico denso de un LI para poder desarrollar racionalmente nuevos electrolitos que podrían estar formados por un LI dopado con una sal inorgánica. En particular, las sales de alta valencia como aquellas que contienen Mg y Al están siendo investigadas porque podrían llevar a sistemas de almacenamiento de energía más eficientes, además de ser más abundantes y, consecuentemente, más baratas que las que se basan en el litio (Li), la opción preferida para baterías hoy en día. La importancia de otras sales que contienen elementos de alta valencia, como el Zn o el Cr, son también relevantes para aplicaciones electrolíticas. En este contexto, la microestructura de los LIs y, en mayor medida, de sus mezclas con sales de interés electroquímico, es de especial relevancia. Específicamente, muchas de las características particulares de la solvatación de iones en LIs son todavía desconocidas en su mayor parte.

Una de las técnicas más eficientes para estudiar las propiedades microscópicas de sistemas moleculares complejos y para predecir las macroscópicas es la simulación por ordenador. En particular, y dado el alto número de LIs que se pueden producir, teóricamente, estos métodos pueden ayudar a los investigadores a ahorrar tiempo y dinero, puesto que los costes de experimentar virtualmente con LIs son generalmente mucho más bajos que los de realizar estos experimentos en la vida real. Por supuesto, el método computacional empleado debe ser escogido cuidadosamente para proveer resultados fiables que se correspondan con los experimentales, si estos están disponibles. Por suerte, en las últimas décadas, los avances tecnológicos y los esfuerzos investigadores han llevado a la mejora y el desarrollo de poderosas herramientas computacionales, las cuales han sido extensivamente utilizadas para estudiar LIs. A pesar del indudable interés por las características precisas de la coordinación iónica en los LIs, y

a pesar también de haber sido utilizadas extensivamente para analizar las propiedades tanto en “bulk” como en la interfaz de las mezclas con iones monovalentes, ha habido comparativamente muy pocos estudios realizados con simulaciones de dinámica molecular (MD) de disoluciones de sales con cationes de alta valencia en LIs.

En la presente tesis, se ha realizado un estudio computacional de mezclas de LIs con sales de diversa valencia, tanto en condiciones bulk como en la interfaz electroquímica. Nuestro principal objetivo era analizar el mecanismo de solvatación de los cationes de sales de alta valencia en LIs, prestando especial atención a la influencia de la valencia del catión de la sal en la estructura de la mezcla y en los complejos que se forman, además de en el carácter prótico o aprótico del LI. Además, se estudió la transferencia de carga del catión de la sal a un electrodo en un medio con LI. Para ello, se utilizaron principalmente simulaciones MD usando el software libre y de código abierto GROMACS y el campo de fuerzas MD estándar OPLS-AA. Aunque este campo de fuerzas no es polarizable (la implementación de campos de fuerzas polarizables está actualmente bajo estudio), es conocido que provee predicciones estructurales muy precisas y tendencias cualitativamente correctas para las propiedades de transporte. Además, simulaciones basadas en la teoría del funcional densidad (DFT) han sido realizadas para describir los complejos metálicos y la transferencia de carga en la interfaz electroquímica. En este último caso, se utilizaron tres programas DFT: VASP, NWChem y Gaussian. El primero está basado en ondas planas, y hemos elegido utilizar el funcional Perdew-Burke-Ernzerhof (PBE) para realizar los cálculos. Los otros dos, por otra parte, usan bases LCAO (en nuestro caso, 6-31G* o 6-311G**), y hemos decidido emplear el funcional híbrido de tres parámetros de Becke con correcciones debido a Lee, Yang y Parr (B3LYP).

Con la idea de obtener más información sobre la solvatación de cationes divalentes en estos medios iónicos densos, en el Capítulo 2.1 presentamos un análisis detallado de la solvatación (estructura y

dinámica monoparticular) de cationes divalentes de Mg^{2+} y Ca^{2+} en mezclas de sales de estos metales con un LI aprótico (AIL) y un LI prótico (PIL) con anión común: hexafluorofosfato de 1-butyl-3-metilimidazolio ([BMIM][PF₆]) y nitrato de etilamonio (EAN), respectivamente. Además, para probar la precisión del campo de fuerzas empleado en nuestras simulaciones, se realizaron medidas experimentales de la densidad de estas mezclas en todos los casos. La estructura de los sistemas simulados fue estudiada por medio de la densidad, propiedades volumétricas, funciones de distribución radial, números de coordinación y, para el PIL, con la evolución del número de enlaces de hidrógeno en función de la concentración de sal añadida. También se calcularon, para analizar la dinámica monoparticular de diversas especies en la mezcla, la función de autocorrelación de velocidades y la densidad de estados vibracionales (vDOS) de los cationes de la sal disuelta. Nuestro principal objetivo era averiguar los mecanismos de coordinación de los cationes divalentes en LIs bulk y evaluar las diferencias, si había alguna, con los cationes monovalentes. La comparación con valores experimentales de tanto las densidades como de los volúmenes molares aparentes, V_ϕ , resultó en un gran acuerdo, confirmando que el campo de fuerzas empleado es fiable para estas mezclas.^a Tanto la constancia de V_ϕ como el hecho de que su valor es cercano al de la sal cristalina pura independientemente de la concentración de la sal en el LI sugieren que el entorno local de los cationes divalentes permanece aproximadamente constante con la adición de sal, y es similar al de la sal en estado sólido. Las funciones de distribución radial muestran dos modos de coordinación (monodentado y bidentado) para el catión de la sal y los aniones del LI, aunque en la mezcla del PIL con Mg^{2+} , el modo bidentado no está presente. Ambos hechos son consistentes con los cationes de la sal siendo solvatados en las nanoregiones polares del LI puro, cuya estructura no se ve apreciablemente afectada por la adición de sal (como se refleja en la constancia de la vDOS del sistema aunque se añada sal), formando una estructura de pseudorred en las nanoregiones polares que es reminiscente a la de la sal cristalina. Por otra parte, la vDOS

^aEl mismo campo de fuerzas es utilizado en todas las simulaciones MD en esta tesis.

de los cationes de la sal en las mezclas revela que hay tres modos vibracionales posibles en las mezclas con el AIL estudiado, mientras que en las mezclas con el PIL basado en nitratos sólo aparece uno, mostrando así diferentes tipos de coordinación en ambos entornos. Además, no se observó un desplazamiento apreciable de los picos asociados a movimientos vibracionales de los cationes de la sal en su “jaula molecular” con la concentración de la sal, un comportamiento opuesto al de iones en disolución acuosa. Este hecho es otra evidencia más de que el incremento de concentración de la sal modifica muy poco en entorno de los iones divalentes. Por tanto, en este trabajo se concluyó que las características principales de la solvatación nanoestructurada de cationes divalentes en LIs son cualitativamente similares a aquellas en las mezclas análogas con sales monovalentes, excepto por el acoplamiento electrostático en las nanoregiones polares de las mezclas con cationes de más alta valencia, que es relativamente más fuerte en este último caso, provocando así la formación de complejos de solvatación octaédricos, en vez de tetrahédricos.

Una vez que hemos estudiado la estructura de mezclas de LIs y sales divalentes, nuestro siguiente objetivo era lograr una caracterización apropiada de su comportamiento en la interfaz electroquímica. Por ello, en el Capítulo 2.2, incluimos un estudio MD de mezclas de tetrafluoroborato de 1-butyl-3-methylimidazolio ([BMIM][BF₄]) con tetrafluoroborato de magnesio (Mg(BF₄)₂) confinadas entre dos paredes de grafeno paralelas, el primer estudio de este tipo, hasta donde conocemos. La estructura del sistema fue analizada por medio de perfiles de densidad iónica, estructura lateral de la primera capa cerca de la superficie de grafeno, y orientaciones angulares de los cationes de imidazolio. Se calcularon también los perfiles de energía libre para los cationes divalentes de magnesio usando dos métodos distintos para evaluar la altura de las barreras de potencial cerca de las paredes, y los resultados se compararon con los de mezclas del mismo LI y una sal de litio (Li(BF₄)). Se analizó la adsorción preferencial de los cationes de magnesio usando un modelo sencillo, además de ser comparada con la de mezclas que incluían cationes de litio. También

se calculó la vDOS de los cationes de Mg^{2+} cuando se encontraban cerca de las paredes, analizándose así la influencia de la carga de la superficie de grafeno. Se confirmó que incluso las paredes de grafeno neutras tienen un efecto importante en la estructura del líquido, dando lugar a una distribución inhomogénea de carga con perfiles oscilatorios, la llamada doble capa eléctrica, que se extiende hasta ~ 2 nm de la pared, donde se recuperan las distribuciones homogéneas del bulk. Por otra parte, cuando la pared está cargada, se produce una fuerte oscilación de carga, la cual, unida con la fuerte solvatación de los cationes de la sal por los aniones del LI, causa que los cationes de la sal estén más cerca de la pared cargada positivamente que de la cargada negativamente. La estructura lateral de las mezclas cerca de la sal revela que aparecen transiciones de “rayas” promediadas en el tiempo a fases ordenadas con simetría hexagonal al dopar el LI, fenómeno que ya se había reportado previamente para mezclas LI-agua. Además, aparece una estructura 3D de “herringbone” en la interfaz, lo que implica que las primeras capas de la doble capa eléctrica están fuertemente acopladas por interacciones de tipo Coulomb, las cuales son reforzadas por los cationes de la sal introducidos en el sistema. En paredes neutras, la configuración más probable para los anillos de imidazolio del catión es casi paralela a la pared, independientemente de la concentración de sal añadida, aunque cargar la pared cambia claramente esta distribución de orientaciones. El análisis de los perfiles de energía libre de los cationes de la sal cerca de la pared concluyó que los cationes divalentes parecen encontrarse con barreras más altas que los monovalentes cuando se aproximan al electrodo, un hecho que también se refleja en los cálculos de la adsorción preferencial de ambos cationes de la sal. Las vDOS de los mismos revelan un desplazamiento al rojo de los picos con respecto a aquellos de las mezclas bulk, lo que implica que los cationes de la sal están menos fuertemente ligados en sus jaulas en la región de la interfaz que en el bulk, un comportamiento opuesto al de las moléculas de agua en LIs. La principal conclusión de este trabajo es que los cationes divalentes tienen más dificultades para alcanzar la interfaz electroquímica que sus contrapartidas monovalentes, debido a las más altas barreras de po-

tencial con las que se topan, causadas por los complejos de solvatación tan estables que son capaces de formar estos cationes metálicos.

Hasta ahora, los AILs, que son conocidos por formar enlaces de hidrógeno débiles, han dominado las aplicaciones electroquímicas a costa de aquellos que forman enlaces de hidrógeno más fuertes (los PILs), aunque en los últimos años el uso de estos últimos parece haber ganado más interés. Sin embargo, a pesar de la vital importancia del enlace de hidrógeno en la microestructura de los LIs y sus mezclas, hasta donde sabemos, no se ha publicado ningún estudio computacional de PILs mezclados con sales 1:1 o 2:1 en la interfaz electroquímica. El trabajo en el Capítulo 2.3 intenta cubrir ese hueco realizando simulaciones de mezclas de nitrato de etilamonio (EAN) con nitratos de litio y magnesio, confinados entre dos paredes de grafeno paralelas (tanto neutras como cargadas). Para analizar la influencia tanto de la valencia del catión de la sal, como la de los enlaces de hidrógeno (usando un PIL que forma fuertes enlaces de hidrógeno), y como la de la carga de la pared sobre la estructura de la doble capa eléctrica en la interfaz electroquímica, se calcularon los perfiles de densidad molecular, las orientaciones angulares de los cationes del LI y la estructura lateral de la capa más cercana a la pared de grafeno de la doble capa eléctrica. También realizamos un análisis dinámico, calculando la vDOS de los cationes de la sal cerca de las paredes de grafeno, que fue comparada con la correspondiente a las mezclas bulk. Finalmente, se investigó la estructura del sistema que contenía nitrato de litio en la interfaz usando cálculos DFT *ab initio*. La orientación angular de los cationes del LI revela que la principal diferencia con las mezclas apróticas sin enlaces de hidrógeno es la preferencia de los cationes en estas últimas a permanecer paralelas a la pared en el caso neutro, debido a la diferente simetría del catión, y la existencia de un rango más amplio de orientaciones en las situaciones cargadas. El análisis de la estructura lateral de la mezcla de sal y PIL revela que los enlaces de hidrógeno inducen zonas polares y apolares más marcadas. La comparación de las vDOS para los cationes monovalentes y divalentes cerca de las paredes muestra un desplazamiento al rojo asociado al

único modo vibracional con respecto al de las mezclas bulk con litio, aunque este desplazamiento está ausente en el caso de las mezclas con magnesio. Todos estos resultados llevan a concluir que los cationes de la sal en medios próticos son capaces de alcanzar más fácilmente la pared cargada negativamente que los mismos cationes en el AIL estudiado, aunque en el mismo tipo de LI, una más alta valencia del catión metálico implica un mayor acoplamiento en los complejos de solvatación y, por tanto, más dificultades para alcanzar las paredes electroquímicas. Nuestros resultados DFT sugieren que las principales diferencias entre las cargas de los cationes de la sal cerca de la pared y las cargas clásicas calculadas mediante MD podrían ser importantes para el comportamiento del sistema y, por tanto, un estudio más preciso de la transferencia de carga es necesario.

Por otra parte, a pesar del creciente interés en las aplicaciones electroquímicas potenciales de aluminio y LIs en baterías, la microestructura de las mezclas de sales trivalentes con estos disolventes iónicos densos es completamente desconocida. En este trabajo (Capítulo 2.4), completamos el estudio de LIs dopados con sales de interés electroquímico estudiando la solvatación de una sal de aluminio en un PIL con anión común. Para este propósito, se realizaron simulaciones MD de mezclas de un PIL, EAN, con nitrato de aluminio ($\text{Al}(\text{NO}_3)_3$), tanto en bulk como confinadas entre paredes de grafeno. Se calcularon varias magnitudes estructurales del sistema, como las densidades, funciones de distribución radial, factores de estructura, números de coordinación y enlaces de hidrógeno para las mezclas bulk, además de los perfiles de densidad iónicos para las mezclas confinadas. Las vDOS para los cationes de la sal, en ambas situaciones, fueron también calculadas. Los resultados obtenidos fueron analizados y comparados con los de mezclas de EAN con sales monovalentes y divalentes, con la intención de estudiar la influencia de la alta carga del catión de la sal en las propiedades del sistema. Por último, se realizaron cálculos DFT *ab initio* para analizar la estructura de los complejos Al^{3+} -ligando, cuyas predicciones para el espectro Raman se compararon con el correspondiente espectro experimental, además

de con el calculado mediante simulaciones MD. Tanto las densidades experimentales como el espectro Raman tienen un buen acuerdo con los resultados experimentales, confirmando que la parametrización de nuestro catión de la sal trivalente es fiable. También encontramos que el campo electrostático en la superficie del ion tiene un gran efecto en el tipo de coordinación de los complejos de solvatación de la sal: cuando este se incrementa, el modo de coordinación bidentado se atenúa progresivamente, con lo que en el caso de los cationes de la sal de aluminio, sólo el modo de coordinación monodentado es posible en estos complejos. El factor total de estructura de las mezclas muestra una compresión de las regiones polares de la mezcla debido a las más fuertes interacciones electrostáticas atractivas que aparecen cuando la sal añadida se coloca en ellas (electrostricción), y que la adición de sal de aluminio en el sistema promueve el orden de corto alcance (hecho reflejado en la formación de estructuras estables “solid-like” y complejos en las nanoregiones polares del líquido) en su seno a costa del orden de largo alcance. Sin embargo, este efecto estructural no parece ser sustancial. Tanto los números de coordinación como los cálculos DFT reflejan la formación de complejos de coordinación octaédricos, equivalentemente a lo que sucedía en las mezclas con magnesio. Además, se realizó un análisis detallado del número de enlaces de hidrógeno por molécula en función de la concentración de la sal, que reveló la fuerte resiliencia de la estructura de las regiones polares del LI a la adición de sales de diversos tipos. En las mezclas confinadas, el resultado más relevante es la semejanza entre las sales divalentes y trivalentes, que alcanzan aproximadamente la misma distancia a la pared, la cual es, de todas formas, más grande que la que consiguen los cationes monovalentes en el mismo PIL. Por tanto, en este trabajo concluimos que la estructura de las mezclas de LIs con sales de aluminio es generalmente muy similar a la estructura de las mezclas con sales divalentes, un efecto que podría ser causado por la existencia de nanoregiones polares del LI que acomodan fácilmente la sal añadida formando los correspondientes complejos de solvatación (por ejemplo, complejos de aluminio- NO_3^- octaédricos en mezclas de EAN con $\text{Al}(\text{NO}_3)_3$).

Otro aspecto esencial con respecto a las aplicaciones electroquímicas de estos electrolitos iónicamente densos es la transferencia de carga electrónica de la especie electroactiva a los electrodos. Aunque las simulaciones MD (combinadas con la teoría clásica de Marcus) proveen una imagen promedio útil de esta transferencia de carga, un análisis microscópico adecuado requiere una descripción detallada de las densidades electrónicas de las especies reaccionantes durante el proceso, por lo que es necesario usar métodos de química cuántica. Siguiendo los resultados del Capítulo 2.3, en el Capítulo 2.5 usamos, por primera vez, DFT para analizar la transferencia de carga entre cationes de litio o magnesio y una pared de grafeno en tres situaciones diferentes: en vacío, entre átomos de flúor para simular una sal fundida convencional, y en un LI. Las cargas de todas las especies en el sistema se analizaron en función de la distancia del catión de la sal a la pared en cada situación. En los sistemas que sólo contienen átomos de flúor, estos se mantienen ionizados casi independientemente de la posición del catión de la sal, y la carga de la sal es principalmente transferida a la pared hasta que el átomo de la sal alcanza la distancia donde están colocados los átomos de flúor, donde se enlaza con ellos. A partir de esa distancia no se detecta un incremento de la transferencia de carga a la pared. Por último, la presencia del LI parece llevar a una diferencia significativa en la transferencia de carga, que comienza a distancias más largas que en otros medios, aunque finalmente resulta en el mismo grado de transferencia de carga al electrodo. Se detectó una mayor eficiencia en el proceso de transferencia de carga y mayores potenciales verticales de ionización para la configuración con el metal más cercano al electrodo, mientras que la tendencia opuesta aparece para las afinidades electrónicas verticales, confirmando así que el intercambio electrónico en la región nanoconfinada cercana al electrodo es energéticamente favorable. Finalmente, no se encontraron diferencias relevantes entre los cationes de la sal monovalente y divalente con respecto a la transferencia de carga. Todos estos resultados sugieren un cierto efecto catalizador de los LIs en la transferencia de carga metal/electrodo en estos medios iónicos densos.

Esta tesis finaliza con un breve resumen de las conclusiones principales y potenciales tendencias futuras, además de con una lista de sus publicaciones relacionadas.





Agradecimientos

Durante estos más de cuatro años de tesis, ha habido un sinfín de momentos y de personas cuyas contribuciones positivas a mi vida no quería dejar de reflejar. Esta tesis es también, en cierta medida, suya. Seguramente podría llenar hojas y hojas de agradecimientos a toda la gente con la que he interactuado estos años, pero puesto que la memoria computacional que debe contener este archivo es finita, los he sintetizado en los siguientes:

- A mi familia, por su apoyo moral y económico, además de su insistencia con los temas académicos, factores sin los que no podría haber llegado hasta aquí.
- A mis directores de tesis, Javier y Luis, por su ayuda científica durante todos estos años, y en especial por las correcciones de las “cuestiones de estilo” que han contribuido enormemente a realzar la calidad narrativa de esta tesis. También por las interesantes conversaciones políticas que han contribuido a una mejor comprensión del mundo por mi parte (aunque mis preferencias sigan siendo las mismas, porque son las mejores para la sociedad en su conjunto).
- A Hadrián y Txema, compañeros investigadores con los que cada día que entré en el despacho aprendí algo nuevo, tanto de Física, como de programación, como de cualquier otra “frikada” aleatoria que se les ocurriera ese día.
- Al resto de compañeros del grupo (Trini, Borja, Julio y Silvia), por sus contribuciones teóricas y/o experimentales a los resultados de esta tesis, además de por sus numerosas enseñanzas científicas.

- A Jesús Carrete, el “señor de los átomos”, por su ayuda durante toda la tesis, y en especial durante la estancia en Grenoble.
- A mis alumnos de Física I y de Mecánica Estadística, que seguramente me han enseñado más que yo a ellos, y con los que he (re)descubierto lo que me divierte poder dar clase, probablemente lo mejor de estos años de tesis.
- A Lumos Compostela, por conseguir sacarme de mi silla sedentaria de investigador computacional y hacer que me ejercitara físicamente, además de por los buenos momentos vividos, tanto dentro como (sobre todo) fuera del campo.
- A mis amig@s. Sobran las palabras. Gracias a tod@s por aguantarme con mis “frikadas”, mis problemas, mis chistes malos y, en definitiva, con todos mis defectos. Espero no olvidarme de ninguno: gracias a Dre, Lucía, Alicia, Alberto, Santi, Izan, Julieta, Fafi, Rosa, y a tod@s los que en algún momento me sacasteis una sonrisa en estos cuatro años.
- Y, especialmente, a Isaac y Marilina, probablemente las personas más importantes para mí en estos cuatro años, cuyas contribuciones a mi bienestar físico y mental no pueden ser expresadas con palabras. Os quiero y os valoro incluso más de lo que creéis.

También deseo agradecer al Centro de Supercomputación de Galicia (CESGA) las numerosas horas de procesador puestas a mi disposición, y al Ministerio de Educación su financiación de esta tesis mediante una beca del programa de Formación de Profesorado Universitario (FPU). La tesis fue realizada con las ayudas de los proyectos AGRUP2015/11, GRC ED431C 2016/001 y ED431D 2017/06 (Xunta de Galicia), y de los proyectos MAT2014-57943-C3-1-P, MAT2014-57943-C3-2-P, MAT2014-57943-C3-3-P, MAT2017-89239-C2-1-P, MAT2017-89239-C2-2-P, CTQ2015-65816-R y FIS2014-59279-P (Ministerio de Economía e Innovación) y FIS2012-33126 (Ministerio

de Ciencia e Innovación); todos estos proyectos fueron financiados parcialmente con fondos FEDER. Las acciones COST CM1206 y MP1303 (Unión Europea) también financiaron esta tesis.





Al humor, la libertad y el cariño





Contents

1	Introduction	1
1.1	Motivation and purpose	1
1.2	Ionic liquids	7
1.3	Methodology	13
2	Results and discussion	25
2.1	Molecular dynamics simulations of the structure and single-particle dynamics of mixtures of divalent salts and ionic liquids.	28
2.2	Molecular dynamics simulation of the structure and interfacial free energy barriers of mixtures of ionic liquids and divalent salts near a graphene wall.	30
2.3	Molecular dynamics simulations of the structure of mixtures of protic ionic liquids and monovalent and divalent salts at the electrochemical interface.	51
2.4	Solvation of Al^{3+} cations in bulk and confined protic ionic liquids: a computational study.	81
2.5	A density functional study of charge transfer at the graphene/ionic liquid interface.	110
3	Conclusions and perspectives	129
	Bibliography	131
	List of Tables	157
	List of Figures	158
	List of publications related to this thesis	165



1 Introduction

1.1 MOTIVATION AND PURPOSE

Without any doubt, energy harvesting and storage has been one of the most important scientific and technological challenges throughout human history. In the last decades, the importance of this topic has been further reinforced due to the much greater complexity of our contemporary civilization, as well as the increasing ecological awareness, which tries to lead to a “decarbonization” of the economy. The energy sources and storage systems of the future must be efficient, sustainable and clean, using new materials that allow significant improvement of these properties relative to their current state of the art. In this context, electrical energy storage has become a major scientific challenge in the last decades.

In particular, development of electrochemical and electrostatic devices translates into several applications useful in our everyday life, such as batteries, supercapacitors, fuel cells, thermoelectrochemical cells, actuators and solar cells. Among the most promising materials for all these purposes, ionic liquids (ILs) stand out. The interest for these new “materials of the future”¹ has been increasing in the past 20 years. In fact, the number of publications related to this topic has been steadily increasing lately, as it is shown in Fig. 1.1. We will deeply dive into the peculiar characteristics of these materials in the following section.

On the other hand, the most relevant and iconic electrochemical device in our society is probably the battery, which consists in one or more electrochemical cells, where chemical energy is converted into electrical energy. Currently, the most used batteries are based on

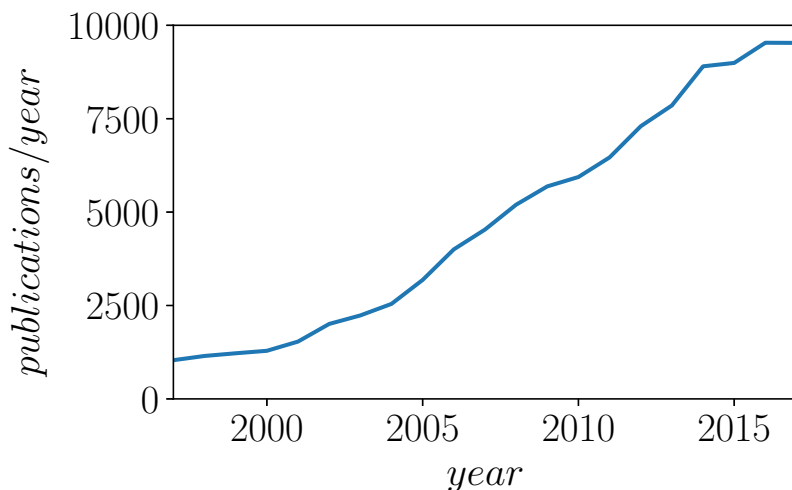


Figure 1.1: Number of publications per year in the past 20 years related to ILs. Data extracted from Web of Science.

lithium, usually containing an electrolyte based on a compound of this element mixed with an organic solvent (e.g. carbonates). This electrolyte is a crucial part of the battery regarding its performance as, together with the electrode, it sets the cell voltage, capacity, coulombic efficiency and cycling stability of the device,² so improving it can lower the cost and enhance the power of the device. However, both the solute and the solvent of currently used electrolytes pose significant challenges. On one hand, lithium is a relatively scarce element on our planet, and some geopolitical factors might additionally hinder its supply and complicate the economics of lithium-based devices. For that reason, it would be convenient to change this metal for some other more easily accessible ones (sodium, potassium, magnesium, calcium and aluminium, among others), and, therefore, cheaper, while preserving the relevant qualities of the battery. On the other hand, conventional organic solvent pose certain problems (high toxicity, great volatility or non biodegradability), which could also be reduced

using alternative solvents. In fact, ILs generally do show the opposite properties: low vapor pressure, low toxicity and biodegradability, while exhibiting the largest electrochemical windows and thermal stabilities of currently known liquid solvents. Taking into account both factors, the study of mixtures of ILs with salts of electrochemical interest (specially those of high valence), which could, in theory, be used as efficient electrolytes in batteries, is extremely relevant regarding the final goal of improving these technological devices.

Although experimental studies of these systems are obviously very necessary before any practical application, computational studies can provide cheaper, and somehow deeper, insight into the behaviour of these systems. In fact, several computational studies related to ILs have been reported in the past years (see Chapter 2 of this thesis for relevant references). Of course, all simulation aspects (force field, simulation conditions, stabilization times, etc.) must be carefully evaluated, and the predictions compared to experimental results in order to check their validity. However, the advantages of computational calculations outnumber their disadvantages, providing a direct microscopic picture of the studied systems and helping to establish a structure-property relationship for them. This knowledge could open the door in the future to the smart design of better ILs or mixtures of ILs with salts that would greatly improve state-of-the-art electrolytes regarding their usage in batteries.

In fact, a tremendous research of experimental and computational effort has been devoted to the use of ILs in these devices, most of them focused on mixtures with salts of lithium or other alkali metals.^{3–24} However, for these applications, a much deeper knowledge of the mechanisms of ion solvation and transport in these environments is still needed. On the purely theoretical side, these phenomena have been considered in the context of the so-called nanostructured solvation,^{25–27} and a pseudolattice theory which accounts for the properties of ionic fluids throughout all the concentration range has emerged as the unifying theoretical framework for these densely ionic solvents.²⁸

Nanostructured solvation and pseudolattice theory give rise to the theoretical framework of this thesis.

Interfacial properties of ILs are also extremely relevant to provide a detailed picture of their behaviour in actual electrochemical devices. In fact, ILs at interfaces feature interesting properties caused by the formation of a highly structured electrical double layer,^{29–43} due to overscreening or crowding phenomena. Moreover, a 3D structure for the electric double layer formed by ILs at the interface was reported by Kornyshev and Qiao.⁴⁴ In spite of their undoubted interest for elucidating the precise features of ionic nanostructured solvation in these amphiphilically nanostructured media, and despite having been used extensively to analyze bulk^{25,45–50} and interfacial⁵¹ properties of mixtures with monovalent ions, computer simulations of mixtures of ILs and salts with high valency cations at the electrified interface have been very scarcely considered in the literature. The peculiar organization of the densely ionic mixture and the associated nanostructured solvation of ions in this environment are at the origin of the high energy barriers for cation transport to the electrochemical interfaces.^{51,52} Some experimental results of mixtures of ILs and 2:1 salts have been reported, in particular about electrodeposition of magnesium,⁵³ coordination complexes of Mg^{2+} cations,⁵⁴ as well as centered in the electrochemical behaviour of magnesium⁵⁵ or cadmium⁵⁶ in ILs. However, to the best of our knowledge, computational studies on mixtures of ILs containing multivalent cations near walls have not been reported so far.

On the other hand, the influence of a hydrogen bonding network on the structure of the IL is another very relevant topic (see, for example, Refs. 57 and 58). However, most of the above mentioned studies are centered in mixtures with AILs, which tend to form weaker hydrogen bonds, although in the last few years the use of strongly hydrogen-bonded PILs in electrochemistry seems to have gained more interest.^{21,59–62} Studies for higher salt cation valencies, such as aluminium-based salts, in ILs, have been focused in electrodeposition^{63–65}

or lubrication mechanisms,^{66,67} although some works concerning aluminium-ion batteries using an IL-based electrolyte have been also reported.^{68,69}

Another phenomenon of special relevance in electrochemical applications is the charge transfer from the salt cation to the electrode. Up to now, most of the theoretical efforts devoted to the description of this phenomenon have been done using MD simulations and in the framework of the classical Marcus theory,⁷⁰ which focuses on the description of the influence of solvent fluctuations on the rate of electron transfer, and whose applicability in bulk ILs was originally proved by Lynden-Bell in 2007.^{71,72} Ten years later, Salanne and coworkers took a step further and studied electron transfer reaction in nanoconfined mixtures of Fe with ILs.⁷³ However, quantum chemical methods are better suited to study this phenomenon, as we can consider explicitly the electronic effects that affect the reacting species during the charge transfer process. In fact, several studies of charge transfer using DFT have been performed,^{74–78} and several DFT studies related to ILs with lithium additives of electrochemical interest have been reported, regarding their adsorption,^{79–81} electrochemical stabilities,^{82–84} and the chemical decomposition of the IL species.^{85–88} However, up to our knowledge, no *ab initio* simulations of charge transfer in ILs have been reported.

This thesis tries to contribute to the study of these electrochemically relevant systems using computational simulations in order to get insight into several structural and dynamical properties of mixtures of ILs with inorganic salts with common anion, both in bulk conditions and confined between graphene walls (charged and uncharged), in order to better approximate the behaviour of the system in an actual battery. Indeed, the **key goals for this thesis** are to provide a deeper understanding in the solvation mechanisms for multivalent salts in ILs, both in bulk conditions and at the electrochemical interface, by analyzing the structural properties and single particle dynamics of the mixtures, paying special attention to the formation of solvation

complexes and the influence of the salt valency on all properties of the system as well as on the charge transfer from the salt cation to an electrode in an IL environment. The main computational tool used for this purpose was classical molecular dynamics, although in order to analyze in a more precise way the structure of some salt complexes formed in the mixtures and the charge transfer from the salt cation to the wall, quantum *ab initio* density functional theory (DFT) simulations were also performed.

All the studies carried out in this thesis reveal that the influence of the salt cation valence on the structure of the pure IL is generally limited, confirming that the solvation of salt cations takes place by means of a nanostructured solvation in the polar zones of the IL. However, increasing valence leads to more resilient molecular cages around salt cations (more stable solvation complexes), hence hindering further their approaching to negatively charged electrodes. Our contribution to the study of trivalent salt cations in ILs reveals a great similarity of the structure of these mixtures with the analogous mixtures with divalent ones in EAN. We now know that ammonium-based PILs and their characteristic hydrogen bonded network allow salt cations to approach the wall closer than those in mixtures with non hydrogen-bonded imidazolium-based AILs. Finally, performing for the first time, up to our knowledge, DFT studies of the electronic charge transfer from the salt cations to the electrode in the densely ionic media, we conclude that this process is catalyzed by these ionic compounds.

The remainder of this chapter is devoted to the main characteristics of ILs and the methodology employed for the computer simulations. In Chapter 2, the results obtained are analyzed and detailedly discussed and, finally, in Chapter 3, we summarize the main conclusions of the thesis and indicate some proposals for further work.

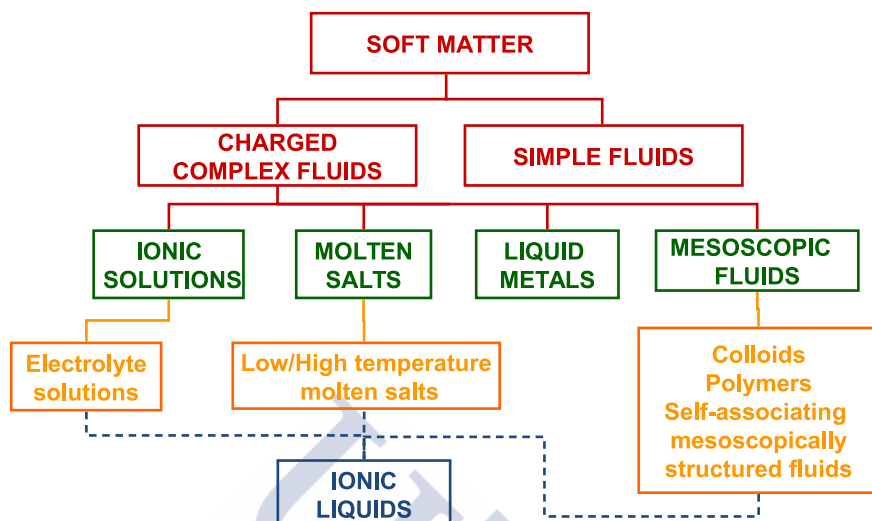


Figure 1.2: Charged fluids comprise most part of soft matter, and ILs are somehow the paradigm of charged complex fluids, because they share properties with most of them, probably except liquid metals, as can be seen in this schematic figure.

1.2 IONIC LIQUIDS

The standard definition of an IL considers it to be a molten salt at room temperature (i.e. melting point below the boiling point of water, 100°). It is precisely because of their nature as molten salts that they are composed entirely by ions, and, seemingly, it is the asymmetry between the anion and the cation of the IL which causes their high melting point. This difference in ion sizes leads to weaker attractive forces and smaller lattice energies between cations and anions than in the case of conventional inorganic molten salts, preventing the formation of a stable lattice structure. Usually, IL anions are small inorganic molecules (in this thesis we deal mainly with NO_3^- , PF_6^- and BF_4^-), while IL cations are normally large organic molecules, being those of the imidazolium, ethylammonium and pyrrolidinium families the most frequently used (in this thesis we will focus on ethylammonium,

[EA]⁺, and 1-butyl-3-methylimidazolium, [BMIM]⁺, cations). In Figs. 1.3 and 1.4, typical IL-forming anions and cations are shown, respectively. The coexistence of organic (apolar) and polar parts in the molecular moieties of ILs confer them an amphiphilic character, which is behind the nanostructuring of these densely ionic solvents.

The very large amount of possible combinations of the currently known anions and cations (10^6 for binary ILs and 10^{18} for ternary ILs, as has been calculated theoretically⁸⁹), as well as the fact that all the properties of these compounds are basically related to their chemical composition, are the reasons why ILs are known as “designer solvents”,⁹⁰ since they can be fine tuned for any particular application. This “tuneability” is precisely the final goal of the studies on ILs: to reach a theory that relates their structure and that of their mixtures with their properties, so an specific IL refined for the needs of any given application could be designed and synthesized. Although producing a new IL can be relatively easy, specific *ab initio* knowledge of their physicochemical properties in order to determine its usefulness is required. For industrial applications this fact is very relevant, but predicting the properties of a given IL from its chemical composition (i.e., an structure-property relation) has not been achieved yet. In this sense, computer simulations, the main methodology used in this thesis, have proved to be essential tools for gaining insight into the connection between the properties of an IL and their structure.

Moreover, ILs have very interesting properties due to their composition. Specifically, combining the appropriate cations and anions we can achieve variable degrees of the following properties:^{91–93}

- **Very low volatility:** ILs have almost negligible vapor pressure at temperatures up to their thermal decomposition temperatures, which is a direct consequence of the strong coulombic interaction between the ions.
- **Relatively low toxicity and biodegradability:** Most ILs are

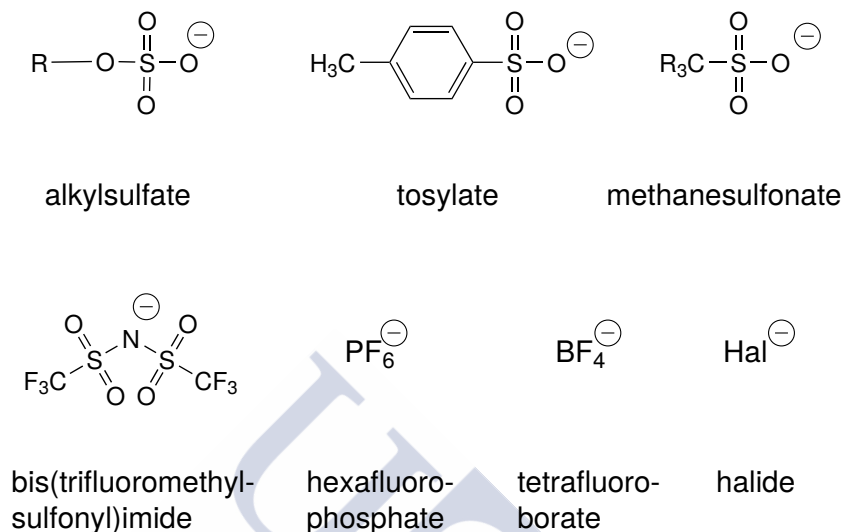


Figure 1.3: Usual anions that form ILs. Reproduced from <http://sigmaaldrich.com>

considered non-polluting and respectful with the environment (as they can be recovered after each use using distillation). This characteristic comes largely from their low volatility that prevents their inhalation, so the only factors of risk would be direct contact with the skin and ingestion, which are much less likely than inhalation. Even so, ILs are frequently irritating for the skin, or toxic if ingested. However, the toxicity can be reduced by appropriately tuning the IL composition. Moreover, some ILs are biodegradable, usually those containing certain functional groups in their composition.⁹⁴ These properties make ILs amphiphilically nanostructured green solvents.

- **High viscosity:** As intermolecular forces in these systems are very intense due to their ionic nature, molecules forming ILs have a low mobility, due to their viscosity being relatively high (from 10 cP up to 500 cP), much higher than that of water (0.890 cP). This magnitude depends strongly on temperature and on

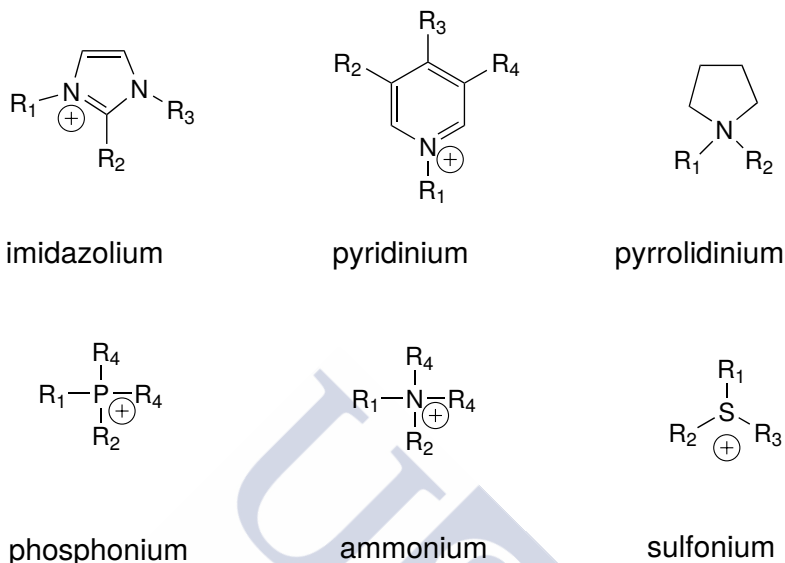


Figure 1.4: Usual cations that form ILs. Reproduced from <http://sigmaaldrich.com>

the presence of impurities.

- **Great thermal stability:** Contrary to what happens with conventional molecular solvents, ILs are in liquid state in a wide temperature range. This characteristic, joined to their low volatility, makes them optimal candidates to be used as thermal fluids.
- **High ionic conductivity and high electrochemical stability:** Both these properties are pivotal for the use of ILs as electrolytes in devices such as batteries, supercapacitors or fuel cells, as it has been pointed out in several reviews.^{41,95–97} ILs have a large stability regarding oxidation or reduction (therefore, they must be doped with a salt of electrochemical interest to be used in electrochemical devices), a broad electrochemical window or high stability when exposed to voltage (up to 6 V wide⁹⁸), and their electric conductivity is the largest of pure liquids (except

the liquid metal mercury) usually of the order of 10^{-1} S/m, which is relatively good, halfway between typical metals and that of distilled water (of the order of 10^6 S/m and 10^{-6} S/m, respectively).

- **High density:** ILs are generally denser than water (for example, [BMIM][BF₄] has a density of 1.37 g/cm³ at 20°C, and that of EAN is 1.26 g/cm³ at the same temperature). Furthermore, this property has a low sensitivity to changes in temperature or the presence of impurities.
- **Variable pH:** Depending on its ionic components, ILs can be acid, basic or neutral. In the particular case of a protic IL, as EAN, its behaviour will depend on the presence of other substances, because a PIL is always formed by an acid cation and a basic anion in a protonation reaction.
- **Amphiphilicity and solvent capabilities:** One of the essential characteristics of ILs is the presence of both a polar part (solvophilic) and an apolar one (solvophobic). These polar and apolar regions are heterogeneously ordered as a consequence of the balance between electrostatic and dispersive forces. This is the reason why ILs are nanostructured materials, formed by entangled polar and apolar networks.^{25,99,100} Thanks to this nanostructured nature, ILs are very versatile solvents which are able to dissolve both polar and apolar substances. One of the greatest industrial interests nowadays is to use these compounds, tuning their capability to solvate other substances at will simply by changing their ionic components. Achieving complete solubility or total immiscibility is possible with modifications in their composition,⁸⁹ which is on the basis of their character of “designer solvents”. ILs are currently considered to have largely expanded the class of solvents from previously known ~600 liquids to an *a priori* practically unlimited amount of members.

- **Nanostructured solvation:**²⁷ Nanostructured solvation has been proposed as a sort of “universal solvation mechanism in amphiphilically nanostructured dense ionic solvents”.²⁷ This solvation is based on the high resilience of the pure IL structure to the presence of additives, as the polar and apolar networks are only slightly affected upon doping of a solute. The solute, hence, selectively accommodates in the nanoregions of the amphiphilically nanostructured IL that are more similar to their molecular entities. Following this mechanism, water forms relatively isolated clusters in non hydrogen-bonded AILs until a continuous water network appears when its concentration in the mixture is high. On the other hand, in strongly hydrogen-bonded PILs, it forms hydrogen bonds with the IL ions and mixes with them homogeneously. IL mixtures with alcohols present the same phenomenon, as they do not clearly clusterize because they can mix with both the polar and apolar regions of the IL. Moreover, when ILs are mixed with salts, salt cations and anions form solvation complexes in the polar regions of the pure IL, giving rise to solvation complexes that organize as a solid-like structure reminiscent of the pure crystalline salt.

A particularly relevant classification for ILs arises from their protic or aprotic character. A common method to synthesize ILs is the transference of a proton by a Brønsted acid to a Brønsted base without the presence of any solvent in the process^{101,102} (protonation process). Whether they are synthesized or not by this route divides ILs in those two families: protic ionic liquids (PILs) and aprotic ionic liquids (AILs), respectively. The main structural difference between PILs and AILs is that the former tend to form a stronger hydrogen bond network.^{103,104}

1.3 METHODOLOGY

In this section, we summarize the main aspects of computer simulations, which are the basic tools employed in this thesis for the analysis of the microstructure of bulk and interfacial properties of IL-salt mixtures. Over the last years, a thorough experimental characterization of ILs has been performed. However, even when they cannot replace experimental results, computational studies have several advantages over experimental research. With computer simulations, we can directly “watch” the behaviour of atoms and molecules of the system, and we are also able to calculate macroscopic magnitudes which could be difficult to obtain experimentally. Moreover, simulation studies are progressively becoming cheaper and more efficient with the continuous technological and computational progress. It is important to recall always that computational results are only valid if both the simulation method and our model (e.g. intermolecular potentials, force field parameters, etc., in the case of MD) properly reproduce experimental properties of the studied system.

Particularly, for the study of ILs, the last few years have seen a huge increase of published computational studies of these compounds (see Refs. 105 and 106 for some excellent reviews of simulations of ILs). In Fig. 1.5, several simulation methods and their characteristic length and time scales are shown. For the simulation of most liquid systems in the time scale of 1 ns and length scale between 1 Å and 10 nm, where the processes in which we are interested take place, there are three main simulation methods available: classical Molecular Dynamics (MD), *ab initio* quantum methods (such as DFT and *ab initio* MD), and even Monte Carlo. Below, a brief description of the computational methods employed for the calculations in this thesis, classical MD and DFT, is presented.

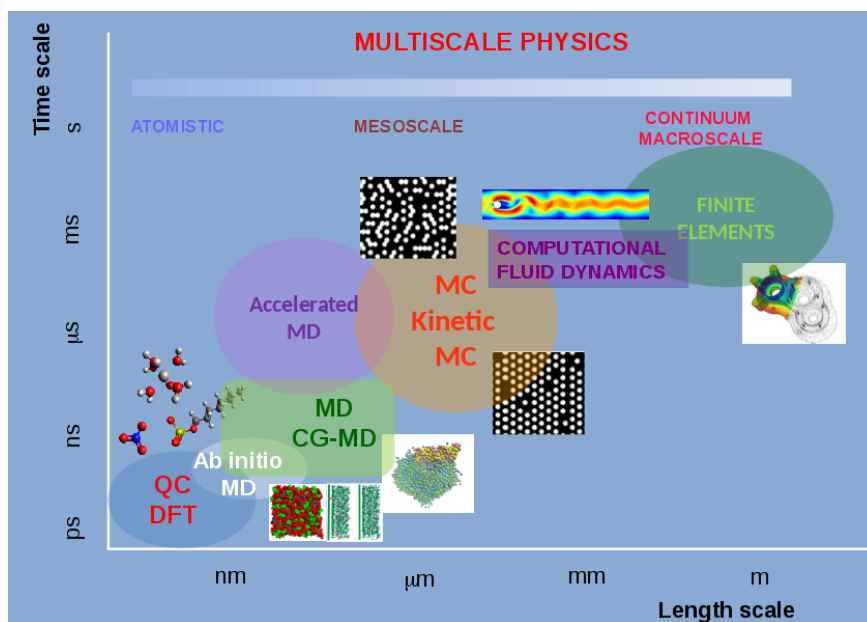


Figure 1.5: Simulation methods and their characteristic time and length scales.

1.3.1 Molecular Dynamics

In this thesis, the most used simulation technique is classical MD, which consists in describing the motion of each atom in the system using the Newton/Lagrange equations of classical dynamics. Modern implementations of MD algorithms (velocity Verlet integration, Nosé-Hoover thermostat and barostat, SHAKE procedure...) in softwares such as LAMMPS or GROMACS benefit from massive parallelization, enabling us to describe systems with thousands of ionic pairs, although some many-body effects such as polarizability or charge transfer are still challenging. In the first simulation stage, the atoms are randomly placed in a virtual box which is replicated in all space dimensions (periodic boundary conditions). This allows simulating a smaller number of atoms in the system without losing statistical accuracy, and,

consequently, saving much computational time, as the properties of the periodic system approach those of a macroscopic system. In the next simulation stage, an initial set of positions and velocities of all the atoms in the system, $\{\vec{r}_i, \vec{v}_i\}$, is generated. These initial velocities are forced to follow Maxwell's distribution at the temperature set for the simulation. After a few minimization and equilibration steps, the system is in a thermodynamical equilibrium. MD simulations use the classical equations of motion in order to calculate the trajectory of positions and velocities for all atoms in the system throughout the chosen simulation time:

$$m_i \frac{d^2 \vec{r}_i}{dt^2} = \vec{F}_i = -\frac{\partial V}{\partial \vec{r}_i}, \quad i = 1 \dots N. \quad (1.1)$$

All MD simulations on this thesis were carried out using the open source GROMACS package,^{107,108} and the initial random configurations of the atoms in the virtual boxes were built using PACKMOL.¹⁰⁹ The integration of Newton's equations of motion is performed using Verlet algorithm,¹¹⁰ where the positions and velocities are calculated at the same value of the time variable:

$$\vec{x}(t + \Delta t) = \vec{x}(t) + \vec{v}(t) \Delta t + \frac{1}{2} \vec{a}(t) \Delta t^2, \quad (1.2)$$

$$\vec{v}(t + \Delta t) = \vec{v}(t) + \frac{\vec{a}(t) + \vec{a}(t + \Delta t)}{2} \Delta t. \quad (1.3)$$

The interactions between all the atoms, which are essential to calculate the MD trajectory from the forces between all atoms in the system, are all included in the force field (or potential), V , employed in the simulation. There are several force fields which are widely used for MD, such as OPLS,¹¹¹ CL&P,¹¹² CHARMM,¹¹³ GROMOS¹¹⁴ and AMBER.¹¹⁵ In the case of the MD simulations of this thesis, the chosen force field was OPLS-AA, which was developed by Jorgensen

for organic liquids, in order to parametrize all the simulated atoms. This potential has the following analytical form shown below:

$$V = V_{bonds} + V_{angles} + V_{dihedrals} + V_{nonbonded}, \quad (1.4)$$

where:

$$V_{bonds} = \sum_{bonds} \frac{1}{2} k_B (r - r_0)^2, \quad (1.5)$$

$$V_{angles} = \sum_{angles} k_\theta (\theta - \theta_0)^2, \quad (1.6)$$

$$V_{torsions} = \sum_{torsions} \frac{1}{2} \{ V_1 [1 + \cos(\phi)] + V_2 [1 - \cos(2\phi)] + V_3 [1 + \cos(3\phi)] + V_4 [1 - \cos(4\phi)] \}, \quad (1.7)$$

$$V_{nonbonded} = \sum_{ij \text{ pairs}} \left\{ 4\epsilon_{ij} \left[\left(\frac{\sigma_{ij}}{r_{ij}} \right)^{12} - \left(\frac{\sigma_{ij}}{r_{ij}} \right)^6 \right] + \frac{q_i q_j}{4\pi\epsilon_0 r_{ij}} \right\}. \quad (1.8)$$

As shown in Eqs. (1.5) and (1.6), the terms that correspond to bonds and angles are represented by harmonic potentials. This is a good approximation because we can usually expect very small oscillations around equilibrium distance (angle) at room temperature. All r_0 , θ_0 , k_i parameters are taken from experimental results. On the other hand, Eq. (1.7) shows that the dihedral torsion potential is represented with a cosine expansion, in which all V_i parameters were calculated using *ab initio* methods. Moreover, the term in Eq. (1.8) shows that all

nonbonding interactions are calculated using Coulomb interactions and a Lennard-Jones potential, which includes both attractive and repulsive van der Waals forces. This Coulomb term is, of course, very relevant in ionic systems, in order to calculate electrostatic long-range interactions. This is frequently done by means of lattice sum methods such as Particle Mesh Ewald (PME),^{116,117} the choice in our calculations. The rest of the relevant force field parameters (such as partial charges or Lennard-Jones σ and ϵ parameters) are generally extracted from first principle quantum mechanical calculations.

Finally, the generated MD trajectory is used to calculate all relevant magnitudes using conventional statistical mechanics methods. In this formalism, the average of a quantity ψ of the system during the simulation time (with contains n discrete time steps), assuming ergodicity of the system, can be written as:

$$\langle \psi \rangle = \langle \psi \rangle_t = \lim_{t \rightarrow \infty} \frac{1}{t} \int_0^t \psi(t') dt' = \lim_{n \rightarrow \infty} \frac{1}{n} \sum_{i=1}^n \psi(t_i). \quad (1.9)$$

All other specific details concerning both the simulation procedure and the postprocessing of results are described in the corresponding section of Chapter 2.

1.3.2 Density Functional Theory

In order to study materials at a quantum level of theory (when the electronic degrees of freedom in the system are essential to properly describe the relevant properties), both the electrons of the system as well as the atomic nuclei must be considered explicitly. The Hamiltonian of these degrees of freedom of such a system must then be written as:

$$\hat{H} = \underbrace{\left[-\frac{\hbar^2}{2m} \sum_i \nabla_i^2 - \frac{1}{4\pi\epsilon_0} \sum_{i,I} \frac{Z_I e^2}{|\mathbf{r}_i - \mathbf{R}_I|} + \frac{1}{8\pi\epsilon_0} \sum_{i,j} \frac{e^2}{|\mathbf{r}_i - \mathbf{r}_j|} \right]}_{\text{electronic part}} - \underbrace{\left[\frac{\hbar^2}{2M} \sum_I \nabla_I^2 + \frac{1}{8\pi\epsilon_0} \sum_{I,J} \frac{Z_I Z_J e^2}{|\mathbf{R}_I - \mathbf{R}_J|} \right]}_{\text{nuclear part}}. \quad (1.10)$$

The essential problem is that, even if we assume that the degrees of freedom of the nuclei can be decoupled from those of the electrons, (Born-Oppenheimer approximation¹¹⁸), trying to solve Schrödinger's equation and obtaining the electronic wavefunction of a system with many electrons collides with the “exponential wall”.¹¹⁹ This causes the computation of wavefunctions for many-electron systems to be non-physical as they would be too demanding for any computational system to calculate and storage with enough accuracy.

A new approximation to the many-body problem of systems with many interacting electrons is then needed. The Hohenberg-Kohn theorems¹¹⁹ state that the external potential $v_{ext}(\mathbf{r})$, and hence the total energy, is a unique functional of the electron density $\rho(\mathbf{r})$, and that the groundstate energy can be obtained variationally: the density that minimises the total energy is the exact ground state density. Although these theorems are extremely powerful and useful, they do not offer a way of computing the ground state density of a system in practice. For this, Kohn and Sham stated that an equivalent system can be built which gives the same charge density, but formed by fictional non-interacting electrons.¹¹⁹ The resulting Kohn-Sham equations can be written as:

$$\left(-\frac{\hbar^2}{2m} \nabla^2 + v_{eff}(\mathbf{r}) \right) \phi_i(\mathbf{r}) = \varepsilon_i \phi_i(\mathbf{r}), \quad (1.11)$$

where ϵ_i is the orbital energy of the corresponding Kohn–Sham orbital, ϕ_i , and the density for an N-particle system is:

$$\rho(\mathbf{r}) = \sum_i^N |\phi_i(\mathbf{r})|^2. \quad (1.12)$$

This implies that the total energy of the system, $E[\rho]$, can be written as follows:

$$E[\rho] = T_s[\rho] + \int d\mathbf{r} v_{ext}(\mathbf{r})\rho(\mathbf{r}) + E_H[\rho] + E_{xc}[\rho], \quad (1.13)$$

where T_s is the Kohn–Sham kinetic energy, v_{ext} the external potential acting over the interacting system, E_H is the Coulomb energy and E_{xc} is the exchange and correlation energy, which includes, amongst other effects, the consequences of the spin-statistics theorem. This theory is formally exact, although the E_{xc} functional is unknown. Nevertheless, there are several approximate families of functionals that work well: LDA, GGA, hybrid functionals... (see e.g. Ref. [120](#) for an excellent review). The most frequently used ones are the following:

- **Local Density Approximation (LDA):** It assumes that charge density changes spatially very slowly, so, inside each small volume, can be approximated by an homogeneous gas of electrons:

$$E_{xc}^{\text{LDA}}[\rho] = \int \rho(\mathbf{r})\epsilon_{xc}[\rho] d\mathbf{r}, \quad (1.14)$$

where ϵ_{xc} is the exchange-correlation energy per particle of the electron gas.

The main problem of LDA is overbinding: the predicted bonding energies are too high, while the predicted bond distances are too low. One of the most often used LDA functionals is the PZ (Perdew and Zunger) functional.¹²¹

- **Generalized-Gradient Approximation (GGA):** It is based on a density gradient expansion: it uses both the density and its gradient at each point:

$$E_{xc}^{\text{GGA}}[\rho] = \int \rho(\mathbf{r}) \epsilon_{xc}[\rho, \nabla \rho] \, d\mathbf{r}. \quad (1.15)$$

Sometimes, this improves the predictions on the bonding and dissociation energies with respect to LDA, but other times it may lead to underbinding. One relevant GGA functional is PBE (Perdew-Burke-Ernzerhof),¹²² which is used in this thesis for some DFT calculations.

- **Meta-GGA:** These functionals include the kinetic energy density, in addition to both the density and its gradient:

$$E_{xc}^{\text{GGA}}[\rho] = \int \rho(\mathbf{r}) \epsilon_{xc}[\rho, \nabla \rho, \nabla^2 \rho] \, d\mathbf{r}. \quad (1.16)$$

They are able to improve the accuracy of bond energies and distances in DFT calculations, a fact which increased their usage in the last few years. One example of an often used Meta-GGA functional is SCAN.⁶⁸

- **Hybrid functionals:** They are based on a combination of an explicit functional of density (either LDA or GGA) with an empirical fraction of exact exchange from Hartree-Fock theory.¹¹⁹ They improve the prediction of some properties like the electronic band gap. One of the most popular ones is B3LYP (Becke, three-parameter, Lee-Yang-Parr),^{123,124} which is used in this thesis for some DFT calculations, and can be written as:

$$E_{xc}^{B3LYP} = E_x^{LDA} + E_c^{LDA} + a_0(E_x^{HF} - E_x^{LDA}) + a_x(E_x^{GGA} - E_x^{LDA}) + a_c(E_c^{GGA} - E_c^{LDA}), \quad (1.17)$$

where $a_0 = 0.20$, $a_x = 0.72$ and $a_c = 0.81$ are empirical parameters.

In DFT calculations, the Kohn-Sham equations are solved by direct minimization of the DFT functional (see Fig. 1.6 for more details on this calculation). Once we solve these equations, we can obtain, among other relevant quantities, the total energy in the ground state and the corresponding atomic positions, forces acting on atoms, charge density, atomic charges, band structures and densities of states.

One last relevant consideration for DFT simulations are the basis functions in which the wavefunction is expanded by the computational method:

$$\psi(\mathbf{r}) = \sum_i c_i \phi_i(\mathbf{r}). \quad (1.18)$$

There are two main classes of basis functions for DFT calculations, each one with its own advantages and disadvantages:

- **Linear combination of atomic orbitals (LCAO):** Wavefunctions of the system are described as a sum of orbitals very similar to the atomic ones. Gaussian basis are often used in quantum chemistry for the study of molecules, but they depend on the atomic position and have superposition errors which might be important for some systems. Both NWChem¹²⁵ and Gaussian,¹²⁶ two packages used in this thesis, use LCAO.

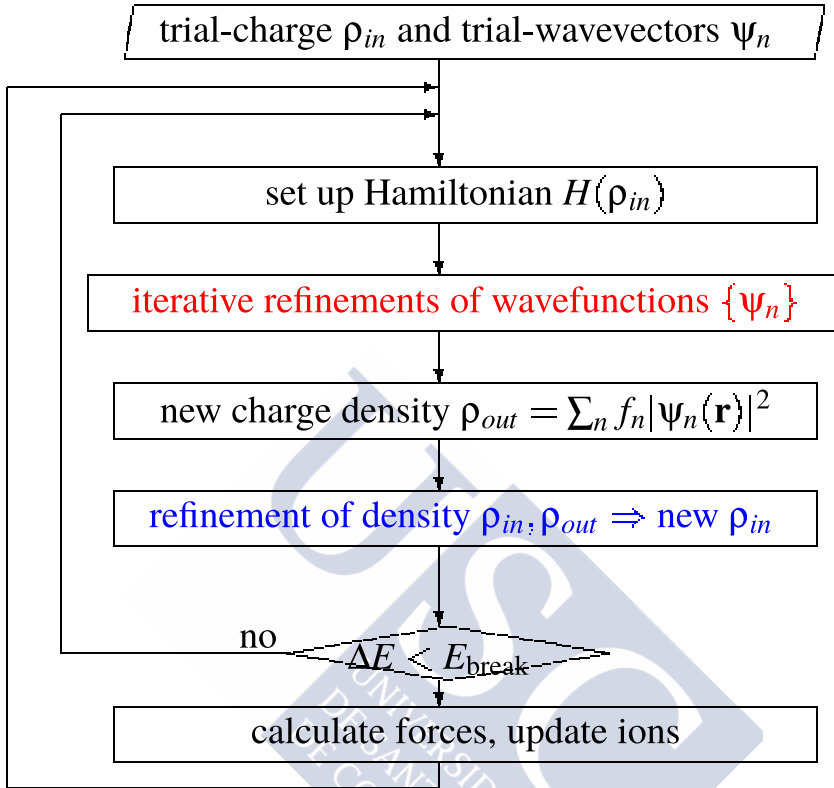


Figure 1.6: Selfconsistency scheme for DFT calculations. Reproduced from <https://www.vasp.at/vasp-workshop/slides/optelectron.pdf>.

- **Plane waves:** Wavefunctions are described as a sum of plane waves far enough from the nuclei, and by some kind of atomic orbitals in the region where the wavefunctions change too fast for that hypothesis to be valid. This basis set is very good for periodic systems such as crystals. The main advantage is their completeness and unbiasedness, as there is only one convergence criteria: cutoff energy (number of plane waves used). The main disadvantage is that this number is very high and that, in non periodic systems, regions where the charge density is very small must be considered, compromising the efficiency

of the method. In this thesis, when required to perform plane wave calculations, VASP software was used.^{127–130}

Further details for each DFT simulation in this thesis are given in the specific sections of the next chapter.





2 Results and discussion

This chapter includes the full description of the results obtained in this thesis. The common goal of all of them was to get a detailed picture of the structure of mixtures of ILs (buthylimidazolium-based ILs as representatives of non hydrogen-bonded AILs, and EAN as a representative of PILs) with salts of electrochemical interest of diverse salt valences, paying special attention to the solvation mechanism of salt cations. Specifically, lithium, magnesium, calcium and aluminium salts were studied in this thesis, in the framework of nanostructured solvation. All these mixtures were studied in bulk conditions and near neutral, positively charged and negatively charged graphene walls, using mainly MD, but also DFT simulations. Moreover, a study of the charge transfer of a salt atom in these promising electrolytes was studied. Indeed, the key goal of this thesis was to provide a better understanding on the solvation mechanisms for multivalent salts in ILs, by analyzing the formed solvation complexes and their effect on the structure and single particle dynamics of the mixture, considering the influence of the salt valence over the properties of the system and comparing the results with those previously reported for monovalent salts. Moreover, we studied for the first time, up to our knowledge, the charge transfer from the salt cation to an electrode in IL environment using DFT.

More specifically, simulations of bulk mixtures of both PILs and AILs with divalent salts were performed in order to compare the results with those for analogous mixtures with monovalent salts. The solvation of the divalent cations was analyzed by calculating several structural and dynamic properties, including apparent molar volumes, radial distribution functions, coordination numbers, hydrogen bonds, velocity autocorrelation functions and vibrational densities of states. All the calculations are consistent with the presence of divalent cations in locally ordered structures in polar nanodomains of the IL, which

are more ordered and more strongly electrostatically coupled than in the corresponding mixtures with Li^+ .

Following the same path, simulations with mixtures of an AIL with a magnesium salt, confined between parallel graphene walls with diverse surface charge densities, were carried out. The structure of these systems was analyzed using ionic density profiles, lateral structure of the first layer close to the graphene surface, and angular orientations of imidazolium cations. Besides, free energy profiles for salt cations as a function of the distance to the wall and vibrational densities of states were reported. These results indicate that magnesium cations close to the graphene wall have a roughly similar environment than that in the bulk, but they face higher free energy barriers and are less present at the interfaces than their monovalent counterparts, as they have a more stable solvation shell than lithium cations in the same AIL.

Moreover, in order to get a complete picture of the influence of confined mixtures of salts with a PIL, and to investigate the influence of its hydrogen bond network in the structure of the mixture, comparing it to that of the corresponding non hydrogen-bonded AIL mixtures, we performed MD simulations for lithium and magnesium salts, mixed with a PIL that forms strong hydrogen bonds, between parallel graphene walls with different surface charges. Ionic density profiles, angular orientations of ethylammonium cations close to the wall, lateral structure of the first layer close to the graphene wall, and vibrational densities of states for the salt cations close to the walls were calculated. Moreover, DFT was used to investigate the structure of the mixture with lithium salt near the interface. We concluded that the salt cation with the smaller salt valence in the same IL is able to reach shorter distances to the graphene wall, and that the hydrogen bonded network characteristic of PILs allows salt cations to approach the wall closer than the same salt cations in mixtures with imidazolium-based AILs.

Furthermore, MD simulations of trivalent aluminium cations,

Al^{3+} , mixed with a PIL, were performed, both in bulk and confined between graphene walls. Several structural quantities of the system were calculated, such as densities, coordination numbers and hydrogen bonds for the bulk mixtures and ionic density profiles for the confined ones. Moreover, vibrational densities of states were calculated for the salt cations, both in bulk and close to the walls. DFT simulations were also performed in order to analyze both the structure of the aluminium-anion complex and to calculate the Raman spectrum of the mixture. The main conclusion was that $[\text{Al}(\text{NO}_3)_6]^{3-}$ octahedral complexes do not significantly change the properties of the mixtures relative to magnesium-based ones, as the addition of salts led to minor and purely quantitative changes of the structure of the IL and its hydrogen bond network.

Finally, in order to investigate in a more precise way the charge transfer between lithium or magnesium cations to a graphene wall, we carried out DFT simulations of these metal atoms in three different kinds of environments (in vacuum, with fluorine atoms and in an IL), calculating the charge of each species as a function of the distance of the salt cation to the wall, as well as vertical ionization potentials and vertical electron affinities. The results suggested a certain catalytic effect of ILs regarding metal-electrode charge transfer, as these compounds can actually accelerate charge transfer to the electrode in electrochemical devices without an associated change in their behaviour as solvents.

All these studies are presented below in a detailed way. For each of them, we include a brief summary and the corresponding published paper. It must be noted that the reference indicators, as well of those of figures and tables, are integrated with the text; due to which it is possible that the numbers do not correspond to those indicated in the papers.

2.1 MOLECULAR DYNAMICS SIMULATIONS OF THE STRUCTURE AND SINGLE-PARTICLE DYNAMICS OF MIXTURES OF DIVALENT SALTS AND IONIC LIQUIDS.

The electrochemical applications of ILs require a detailed knowledge of the ion solvation and transport. Studies on this matter have been focused in mixtures of ILs with monovalent salts, mainly lithium, which have been shown to fall in the nanostructured solvation paradigm, but there have been very few reports of MD simulations of solutions of salts with high valency cations, which might provide several advantages in their applications to these devices. In Ref. 131, we reported the first, up to our knowledge, MD study of mixtures of ILs with divalent magnesium and calcium salts. Our main goal was to understand the coordination mechanisms of divalent cations in bulk ILs and to analyze their differences, if any, with monovalent cations.

In this work, a detailed analysis of the structure and single-particle dynamics of divalent cations of Mg^{2+} and Ca^{2+} in mixtures of salts of these metals with a non hydrogen-bonded AIL and a PIL (that forms strong hydrogen bonds) with a common anion was performed: 1-butyl-3-methylimidazolium hexafluorophosphate ($[\text{BMIM}][\text{PF}_6]$) and ethylammonium nitrate (EAN), respectively. The comparison with experimental values of both densities and apparent molar volumes, V_ϕ , confirmed that the employed force field, OPLS-AA, was appropriate to study these systems. Radial distribution functions showed two coordination modes for the salt cations solvated by IL anions (monodentate and bidentate). Most of the calculations which were performed suggest that the local environment of the divalent cations remains approximately constant upon the addition of salt, which can only be understood if they are forming a quasi-lattice structure reminiscent of the solid crystalline salt in the IL polar regions. The only relevant difference with monovalent salts was the stronger electrostatic coupling in the polar nanoregions of the mixture, which resulted in the formation of more strongly coordinated solvation complexes.



Molecular dynamics simulations of the structure and single-particle dynamics of mixtures of divalent salts and ionic liquids

Víctor Gómez-González,¹ Borja Docampo-Álvarez,¹ Oscar Cabeza,² Maxim Fedorov,³

Ruth M. Lynden-Bell,⁴ Luis J. Gallego,¹ and Luis M. Varela^{1,a)}

¹Grupo de Nanomateriais e Materia Branda, Departamento de Física da Materia Condensada,

Universidade de Santiago de Compostela, Campus Vida s/n, E-15782 Santiago de Compostela, Spain

²Facultade de Ciencias, Universidade da Coruña, Campus A Zapateira s/n, E-15008 A Coruña, Spain

³Department of Physics, Scottish University Physics Alliance (SUPA), University of Strathclyde,

John Anderson Bldg., 107 Rottenrow East, Glasgow G4 0NG, United Kingdom

⁴Department of Chemistry, University of Cambridge, Lensfield Road, Cambridge CB2 1EW, United Kingdom

(Received 12 July 2015; accepted 14 September 2015; published online 29 September 2015)

[<http://dx.doi.org/10.1063/1.4931656>]

2.1.1 Paper I: Molecular dynamics simulations of the structure and single-particle dynamics of mixtures of divalent salts and ionic liquids; *J. Chem. Phys.* 143(12) (2015) 124507.

Víctor Gómez-González,^a Borja Docampo-Álvarez,^a Oscar Cabeza,^b Maxim Fedorov,^c Ruth M. Lynden-Bell,^d Luis J. Gallego,^a and Luis M. Varela^a

<https://aip.scitation.org/doi/full/10.1063/1.4931656>

^aGrupo de Nanomateriais e Materia Branda, Departamento de Física da Materia Condensada, Universidade de Santiago de Compostela, E-15782 Santiago de Compostela, Spain

^bFacultad de Ciencias, Universidade de A Coruña, Campus A Zapateira s/n, E-15008, A Coruña, Spain

^cDepartment of Physics, Scottish University Physics Alliance (SUPA), University of Strathclyde, John Anderson Bldg., 107 Rottenrow, Glasgow, G4 0NG United Kingdom

^dDepartment of Chemistry, University of Cambridge, Lensfield Road, Cambridge, UK CB2 1EW

2.2 MOLECULAR DYNAMICS SIMULATION OF THE STRUCTURE AND INTERFACIAL FREE ENERGY BARRIERS OF MIXTURES OF IONIC LIQUIDS AND DIVALENT SALTS NEAR A GRAPHENE WALL.

Following the studies in the previous section, and in order to study the behaviour of an IL-based electrolyte for electrochemical applications in more realistic situations, in Ref. 164 we confined mixtures of an AIL of the imidazolium family with a divalent salt with common anion between two parallel graphene walls of different surface charge densities so we could analyze the differences between the structure of these confined mixtures with the analogous ones with monovalent salts and bulk ones.

Indeed, in this work we performed a MD study of mixtures of the AIL [BMIM][BF₄] with Mg(BF₄)₂ confined between two parallel graphene walls. Some of the phenomena which had been previously observed for analogous systems were confirmed, such as the formation of a highly inhomogeneous spatial separation of charge, called electrical double layer, even when the graphene wall was neutral; the strong layering of charge near charged walls (oscillatory profiles of charge densities and electrostatic potentials; overscreening...); or the salt cations being closer to the positively charged wall than to the negatively charged one due to the formation of negatively charged magnesium-anion solvation complexes. The lateral structure of the mixtures near the walls showed transitions from time-averaged stripes to ordered phases with hexagonal symmetry taking place upon doping of the IL, as had been previously reported for IL-water mixtures. Moreover, a herringbone interfacial 3D structure appeared, caused by the electrostatic coupling of the first layers. The orientation of imidazolium cations with respect to the wall was also analyzed, and the most probable configuration for imidazolium cation rings was found to be almost parallel to the wall when it is near a neutral wall. Charging the wall changed the distribution of orientations. The calculation of the preferential adsorption of the salt cations and their free

energy profiles near the wall showed that divalent cations face higher barriers than monovalent ones as they approached the electrodes, due mainly to the more strongly coordinated complexes observed in the previous paper. vDOS for the salt cations revealed a red shift of all the peaks of the normal modes relative to those of the bulk.





PCCP

PAPER

[View Article Online](#)
[View Journal](#) | [View Issue](#)Cite this: *Phys. Chem. Chem. Phys.*,
2017, 19, 846Received 12th October 2016,
Accepted 30th November 2016

DOI: 10.1039/c6cp07002g

Molecular dynamics simulation of the structure and interfacial free energy barriers of mixtures of ionic liquids and divalent salts near a graphene wallVíctor Gómez-González,^a Borja Docampo-Álvarez,^a Trinidad Méndez-Morales,^a Oscar Cabeza,^b Vladislav B. Ivaništšev,^c Maxim V. Fedorov,^{de} Luis J. Gallego^a and Luis M. Varela^{*a}**2.2.1 Paper II: Molecular dynamics simulation of the structure and interfacial free energy barriers of mixtures of ionic liquids and divalent salts near a graphene wall; *Phys. Chem. Chem. Phys.* 19(1) (2017) 846.****Víctor Gómez-González,^a Borja Docampo-Álvarez,^a Trinidad Méndez-Morales,^a Oscar Cabeza,^b Vladislav B. Ivaništšev,^c Maxim V. Fedorov,^{d,e} Luis J. Gallego,^a and Luis M. Varela^a**

<http://pubs.rsc.org/en/content/articlehtml/2017/cp/c6cp07002g>

^aGrupo de Nanomateriales, Fotónica y Materia Blanda. Departamento de Física de Partículas, Facultade de Física, Universidade de Santiago de Compostela, Campus Vida s/n, E-15782 Santiago de Compostela, Spain

^bDepartamento de Física, Facultade de Ciencias, Universidade da Coruña, Campus A Zapateira s/n, E-15071 A Coruña, Spain

^cInstitute of Chemistry, University of Tartu, Ravila 14a, Tartu 50411, Estonia

^dDepartment of Physics, Scottish University Physics Alliance (SUPA), University of Strathclyde, John Anderson Bldg, 107 Rottenrow, Glasgow, G4 0NG United Kingdom.

^eSkolkovo Institute of Science and Technology, Moscow, Russia.

2.3 MOLECULAR DYNAMICS SIMULATIONS OF THE STRUCTURE OF MIXTURES OF PROTIC IONIC LIQUIDS AND MONOVALENT AND DIVALENT SALTS AT THE ELECTROCHEMICAL INTERFACE.

PILs have been gaining more interest in the last few years for electrochemical applications, although, up to now, the most investigated ILs for this purpose are non (or weak) hydrogen-bonded aprotic ones. As the influence of the hydrogen bonding network in the structure of the mixtures is a question of vital importance, and there were no computational studies of the behaviour of neither monovalent nor divalent salts mixed with PILs near an interface, we decided to fill that gap with the study in Ref. 172, with the purpose of analyzing the influence of the salt cation charge, the protic character of the IL, which forms strong hydrogen bonds, and the charge of the interface on the structure of the electric double layer at the electrochemical interface.

In this work, we performed MD simulations of mixtures of a strong hydrogen-bonded PIL, ethylammonium nitrate (EAN), with lithium and magnesium nitrates confined between two parallel graphene walls (both in the neutral and charged states). Angular orientation of IL cations revealed that the main differences with the aprotic mixtures are mainly caused by the shape and charge distribution differences of both IL cations. Lateral structure calculations showed that the effect of hydrogen bonds was to form polar and apolar regions much more marked than in mixtures with non hydrogen-bonded AILs. The comparison of the vDOS for the monovalent cations near the walls showed a red shift of the peak associated to the only possible vibrational mode relative to its value in bulk mixtures, which was not present in the case of mixtures with magnesium. All these results concluded that salt cations in strong hydrogen-bonded protic environments are able to approach more easily the negatively charged wall than the same metal cations in non hydrogen-bonded AILs, although within the same kind of IL a higher salt cation valence implied more difficulty for approach-

ing the interface. DFT results suggested that electronic effects might be important for the “real” charge values of the salt cation-anion complex near the graphene wall, so a complete DFT study of the charge transfer might be necessary (see Chapter 2.5).



PCCP



PAPER

[View Article Online](#)
[View Journal](#) | [View Issue](#)

Cite this: *Phys. Chem. Chem. Phys.*,
2018, 20, 12767
Received 21st February 2018,
Accepted 16th April 2018
DOI: 10.1039/c8cp01180j

Molecular dynamics simulations of the structure of mixtures of protic ionic liquids and monovalent and divalent salts at the electrochemical interface

Víctor Gómez-González,^a Borja Docampo-Álvarez,^a J. Manuel Otero-Mato,^a
Oscar Cabeza,^b Luis J. Gallego^b and Luis M. Varela^{b*}

2.3.1 Paper III: Molecular dynamics simulation of the structure of mixtures of protic ionic liquids and monovalent and divalent salts at the electrochemical interface; *Phys. Chem. Chem. Phys.* 20 (2018) 12767-12776.

Víctor Gómez-González,^a Borja Docampo-Álvarez,^a J. Manuel Otero-Mato,^a Oscar Cabeza,^b Luis J. Gallego,^a and Luis M. Varela^a

<http://pubs.rsc.org/en/content/articlehtml/2018/cp/c8cp01180j>

^aGrupo de Nanomateriales, Fotónica y Materia Blanda. Departamento de Física de Partículas, Facultade de Física, Universidade de Santiago de Compostela, Campus Vida s/n, E-15782 Santiago de Compostela, Spain

^bDepartamento de Física y Ciencias de la Tierra, Facultade de Ciencias, Universidade da Coruña, Campus A Zapateira s/n, E-15071 A Coruña, Spain

2.4 SOLVATION OF Al^{3+} CATIONS IN BULK AND CONFINED PROTIC IONIC LIQUIDS: A COMPUTATIONAL STUDY.

This work tries to complete the studies in Chapters 2.1, 2.2 and 2.3 by doping the IL with a very high valence (3:1) salt. The work in Ref. 178 is the first one which considers, using mainly MD simulations, mixtures of a PIL with an aluminium salt both in the bulk and near graphene walls, with the main goal of analyzing the effect of the high charge density of the ion on the structure of the IL and compare its effects to those of all other salt cations in analogous mixtures (see previous chapters).

Indeed, in this work, MD simulations of mixtures of EAN PIL, with aluminium nitrate ($\text{Al}(\text{NO}_3)_3$), both in bulk and confined between graphene walls, were performed, as well as a brief DFT analysis of the Al^{3+} -ligand complexes that form inside these mixtures. A strong correlation between the electrostatic field at the ion surface and the type of coordination of salt solvation complexes was found. The analysis of the total structure factor of the mixtures showed that the addition of salt does not substantially change the long-range structure of the pure IL. Both coordination numbers and DFT calculations reflected the formation of octahedral coordination complexes between the salt metal cation and the IL anion, similar to those in mixtures of the same IL with magnesium. On the other hand, the study of the evolution of hydrogen bonds as a function of salt concentration reflected the strong resiliency of the IL polar nanoregions to the addition of salts of different valencies. Finally, when these mixtures were placed near a graphene wall, their behaviour was also very similar to that of the corresponding mixtures with divalent salts. All these results suggest that the PIL can successfully host metal cations without undergoing strong disordering of their essential structure.

PCCP



PAPER

View Article Online
View Journal | View Issue

Cite this: *Phys. Chem. Chem. Phys.*,
2018, 20, 19071
Received 8th May 2018,
Accepted 26th June 2018
DOI: 10.1039/c8cp02933d

Solvation of Al^{3+} cations in bulk and confined protic ionic liquids: a computational study

Víctor Gómez-González,^a Borja Docampo-Álvarez,^a Hadrián Montes-Campos,^{ib}
Juan Carlos Otero,^{ib} Elena López Lago,^{ib} Oscar Cabeza,^{ib} Luis J. Gallego^a
and Luis M. Varela^{ib} *^a

2.4.1 Paper IV: Solvation of Al^{3+} cations in bulk and confined protic ionic liquids: a computational study; *Phys. Chem. Chem. Phys.*, 20 (2018) 19071-19081.

Víctor Gómez-González,^a Borja Docampo-Álvarez,^a Hadrián Montes-Campos,^a Juan Carlos Otero,^b Elena López Lago,^a Oscar Cabeza,^c Luis J. Gallego,^a and Luis M. Varela^a

<https://pubs.rsc.org/en/content/articlehtml/2018/cp/c8cp02933d>

^aGrupo de Nanomateriales, Fotónica y Materia Blanda. Departamento de Física de Partículas y Departamento de Física Aplicada, Facultade de Física, Universidade de Santiago de Compostela, Campus Vida s/n, E-15782 Santiago de Compostela, Spain

^bUniversidad de Málaga, Andalucía Tech, Facultad de Ciencias, Departamento de Química Física, Unidad Asociada CSIC, 29071-Málaga, Spain

^cDepartamento de Física y Ciencias de la Tierra, Facultade de Ciencias, Universidade da Coruña, Campus A Zapateira s/n, E-15071 A Coruña, Spain

2.5 A DENSITY FUNCTIONAL STUDY OF CHARGE TRANSFER AT THE GRAPHENE/IONIC LIQUID INTERFACE.

Following the results from Chapters 2.2 and 2.3, we decided to gain deeper insight into the charge transfer from the electroactive species to the electrode when it is placed near an IL media, as this is an essential subject in electrochemical devices. This had been studied previously in the framework of classical Marcus theory using MD simulations. However, classical simulation methods do not properly consider the electronic densities, but in an average fashion, so in Ref. 196 we used DFT simulations to have a clear information on the charge transfer process.

In this work, and for the first time, DFT was performed in order to study the charge transfer between lithium or magnesium atoms and a graphene wall in three different situations: in vacuum, amongst fluorine atoms to simulate a molten salt, and in an IL. Charges of all the species in the system as a function of the distance of the salt atom to the wall in each of the three situations were analyzed. In the F system, these atoms remain completely ionized throughout all salt atom positions, while both Li and Mg transfer their charges to the wall at large distances, before they approach fluorine atoms, where they bond to the latter and stop transferring the charge. When the salt is in an IL environment, this compound accelerates the charge transfer process without altering its nature, thus working as a somehow catalyst of the charge transfer. The favorable electronic exchange in the nanoconfined region close to the electrode was confirmed by the vertical ionization potentials and vertical electronic affinities. No relevant difference between monovalent and divalent cations was found regarding the charge transfer.

Density Functional Study of Charge Transfer at the Graphene/Ionic Liquid Interface

V. Gómez-González,[†] A. García-Fuente,[‡] A. Vega,[§] J. Carrete,^{||} O. Cabeza,[⊥] L. J. Gallego,[†]
and L. M. Varela^{*,†}

Received: March 23, 2018

Revised: June 8, 2018

Published: July 2, 2018

2.5.1 Paper V: A density functional study of charge transfer at the graphene/ionic liquid interface; *J. Phys. Chem. C*, 122 (2018) 15070-15077.

Víctor Gómez-González,^a Amador García Fuente,^b Andrés Vega,^c Jesús Carrete,^d Oscar Cabeza,^e Luis J. Gallego,^a and Luis M. Varela^a

<https://pubs.acs.org/doi/abs/10.1021/acs.jpcc.8b02795>

^aGrupo de Nanomateriais, Fotónica e Materia Branda, Departamento de Física de Partículas, Universidade de Santiago de Compostela, Campus Vida s/n E-15782, Santiago de Compostela, Spain

^bDepartamento de Física, Universidad de Oviedo, E-33007 Oviedo, Spain

^cDepartamento de Física Teórica, Atómica y Óptica, Universidad de Valladolid, E-47011 Valladolid, Spain

^dInstitute of Materials Chemistry, TU Wien, A-1060 Vienna, Austria

^eGrupo Mesturas, Departamento de Física e Ciencias da Terra, Universidade de A Coruña, Facultade de Ciencias, Campus A Zapateira s/n E-15012, A Coruña, Spain



3 Conclusions and perspectives

The main conclusions that follow from the papers reported in the previous chapters, regarding the objectives of this thesis, are:

1. In order to use ILs as electrolytes in electrochemical devices, the study of mixtures of a PIL and imidazolium-based AILs with salts of different valency (lithium, magnesium, calcium and aluminium) has been performed using mainly MD simulations, supplemented by DFT calculations. The studies were carried out both for bulk mixtures and for mixtures confined between graphene walls (neutral, positively charged, and negatively charged). In the studied cases, salt cations are seen to be placed in the polar nanoregions of the IL and solvated by anions according to the predictions of the nanostructured solvation paradigm, without appreciably affecting the structure of the polar nanoregions. This solvation mechanism was reflected in several of the calculated properties of the system, but specially in the constancy throughout all salt concentrations of the partial molar volumes of the added salts, which presented similar values to those of the pure crystalline salt.
2. Pioneer calculations for aluminium salts in IL using both MD and DFT were carried out. Tetrahedral salt cation-anion complexes, $[XA_4]^{-4+Z}$, formed for monovalent salt cations were found, while both for divalent and trivalent salt cations octahedral complexes, $[XA_6]^{-6+Z}$, were detected. It seems that similar complexes lead to similar structures of the mixtures, independently of the salt cation valency, as reflected by the high similarity between mixtures of a PIL with magnesium and with aluminium. The coordination types (monodentate or bidentate) in these complexes are related to the electric potential at the surface of the salt cation.

3. Hydrogen bond network in the studied PIL was found to lead to much more marked polar and apolar nanoregions in the structure of the mixtures, compared to those in the considered non hydrogen-bonded AIL. These, in turn, cause the salt cation solvation complexes to be more resilient and allows them to approach more easily the graphene walls than those in the analogous mixtures with AIL, where salt cations can desolvate and transfer their charge to the wall. The MD configurations near the wall were seen to be stable using DFT calculations.
4. On the other hand, within the same kind of IL, monovalent salt cations are able to reach closer distances to the wall than higher valency salt cations, due to the smaller free energy barriers that they have to overcome near the graphene walls with respect to those that higher valency cations face.
5. Finally, the first DFT-based charge transfer analysis of a monovalent and a divalent salt cation in an IL environment was performed. Our results suggested a certain catalysing effect of ILs as regards metal/electrode charge transfer in these densely ionic environments, as the distance at which charge transfer starts in IL environment is around 8 Å while it starts at 4 Å in vacuum. The same final charge for the salt cation is reached in the three environments considered.
6. Regarding future work and perspectives, mixtures of ILs (specially strong hydrogen-bonded PILs) with salts of electrochemical interest and cosolvents might be the next step in order to study the influence of a neutral molecular species on the structure of the complexes, transport, charge transfer and free energy barriers. More precise calculations (probably with *ab initio* MD) of charge transfer from salt cations to the electrode, maybe studying non-graphene materials or intercalating layers of graphene as electrodes, might also be an interesting future direction.

Bibliography

- ¹ K. R. Seddon, "Ionic liquids: a taste of the future," *Nat. Mater.*, vol. 2, no. 6, pp. 363–365, 2003.
- ² L. Suo, O. Borodin, T. Gao, M. Olguin, J. Ho, X. Fan, C. Luo, C. Wang, and K. Xu, "'Water-in-salt' electrolyte enables high-voltage aqueous lithium-ion chemistries," *Science*, vol. 350, no. 6263, pp. 938–943, 2015.
- ³ H. Sakaebe and H. Matsumoto, "N-Methyl-N-propylpiperidinium bis(trifluoromethanesulfonyl)imide (PP13-TFSI) - novel electrolyte base for Li battery," *Electrochem. Commun.*, vol. 5, no. 7, pp. 594–598, 2003.
- ⁴ B. García, S. Lavallée, G. Perron, C. Michot, and M. Armand, "Room temperature molten salts as lithium battery electrolyte," *Electrochim. Acta*, vol. 49, no. 26, pp. 4583–4588, 2004.
- ⁵ W. A. Henderson and S. Passerini, "Phase Behavior of Ionic Liquid-LiX Mixtures: Pyrrolidinium Cations and TFSI-Anions," *Chem. Mater.*, vol. 16, no. 15, pp. 2881–2885, 2004.
- ⁶ M. Diaw, A. Chagnes, B. Carré, P. Willmann, and D. Lemordant, "Mixed ionic liquid as electrolyte for lithium batteries," *J. Power Sources*, vol. 146, no. 1–2, pp. 682–684, 2005.
- ⁷ Q. Zhou, W. A. Henderson, G. B. Appetecchi, and S. Passerini, "Phase Behavior and Thermal Properties of Ternary Ionic Liquid-Lithium Salt (IL-IL-LiX) Electrolytes," *J. Phys. Chem. C*, vol. 114, no. 3, pp. 6201–6204, 2010.
- ⁸ S. Y. Lee, H. H. Yong, Y. J. Lee, S. K. Kim, and S. Ahn, "Two-cation competition in ionic-liquid-modified electrolytes for lithium ion batteries," *Green Chem.*, vol. 109, no. 28, pp. 13663–13667, 2005.

- ⁹ I. Nicotera, C. Oliviero, W. A. Henderson, G. B. Appetecchi, and S. Passerini, "NMR Investigation of Ionic Liquid–LiX Mixtures: Pyrrolidinium Cations and TFSI- Anions," *J. Phys. Chem. B*, vol. 109, no. 48, pp. 22814–22819, 2005.
- ¹⁰ M. Castriota, T. Caruso, R. G. Agostino, E. Cazzanelli, W. A. Henderson, and S. Passerini, "Raman Investigation of the Ionic Liquid N-Methyl-N-propylpyrrolidinium Bis(trifluoromethanesulfonyl)imide and Its Mixture with LiN(SO₂CF₃)₂," *J. Phys. Chem. A*, vol. 109, no. 1, pp. 92–96, 2005.
- ¹¹ J. Lassègues, J. Grondin, and D. Talaga, "Lithium solvation in bis(trifluoromethanesulfonyl)imide-based ionic liquids," *Phys. Chem. Chem. Phys.*, vol. 8, no. 48, pp. 5629–5632, 2006.
- ¹² E. Markevich, V. Baranchugov, and D. Aurbach, "On the possibility of using ionic liquids as electrolyte solutions for rechargeable 5V Li ion batteries," *Electrochem. Commun.*, vol. 8, no. 8, pp. 1331–1334, 2006.
- ¹³ J. Xu, J. Yang, Y. NuLi, J. Wang, and Z. Zhang, "Additive-containing ionic liquid electrolytes for secondary lithium battery," *J. Power Sources*, vol. 160, no. 1, pp. 621–626, 2006.
- ¹⁴ S. Seki, Y. Kobayashi, H. Miyashiro, Y. Ohno, A. Usami, Y. Mita, N. Kihira, M. Watanabe, and N. Terada, "Lithium secondary batteries using modified-imidazolium room-temperature ionic liquid," *J. Phys. Chem. B*, vol. 110, no. 21, pp. 10228–10230, 2006.
- ¹⁵ M. Egashira, H. Todo, N. Yoshimoto, M. Morita, and J. Yamaki, "Functionalized imidazolium ionic liquids as electrolyte components of lithium batteries," *J. Power Sources*, vol. 174, no. 2, pp. 560–564, 2007.
- ¹⁶ Y. Saito, T. Umecky, J. Niwa, T. Sakai, and S. Maeda, "Existing Condition and Migration Property of Ions in Lithium Electrolytes with Ionic Liquid Solvent," *J. Phys. Chem. B*, vol. 111, no. 40, pp. 11794–11802, 2007.

- ¹⁷ V. Borgel, E. Markevich, D. Aurbach, G. Semrau, and M. Schmidt, "On the application of ionic liquids for rechargeable Li batteries: High voltage systems," *J. Power Sources*, vol. 189, no. 1, pp. 331–336, 2009.
- ¹⁸ J. Lassègues, J. Grondin, C. Aupetit, and P. Johansson, "Spectroscopic identification of the lithium ion transporting species in LiTFSI-doped ionic liquids," *J. Phys. Chem. A*, vol. 113, no. 1, pp. 305–314, 2009.
- ¹⁹ B. G. Nicolau, A. Sturlaugson, K. Fruchey, M. C. C. Ribeiro, and M. D. Fayer, "Room temperature ionic liquid-lithium salt mixtures: Optical Kerr effect dynamical measurements," *J. Phys. Chem. B*, vol. 114, no. 25, pp. 8350–8356, 2010.
- ²⁰ Q. Zhou, K. Fitzgerald, P. D. Boyle, and W. A. Henderson, "Phase Behavior and Crystalline Phases of Ionic Liquid-Lithium Salt Mixtures with 1-Alkyl-3-methylimidazolium Salts," *Chem. Mater.*, vol. 22, no. 3, pp. 1203–1208, 2010.
- ²¹ S. Menne, J. Pires, M. Anouti, and A. Balducci, "Protic ionic liquids as electrolytes for lithium-ion batteries," *Electrochem. Commun.*, vol. 31, pp. 39–41, 2013.
- ²² H. Yoon, G. Lane, Y. Shekibi, P. Howlett, M. Forsyth, A. Best, and D. MacFarlane, "Lithium electrochemistry and cycling behaviour of ionic liquids using cyano based anions," *Energy Environ. Sci.*, vol. 6, no. 3, pp. 979–986, 2013.
- ²³ F. Castiglione, A. Famulari, G. Raos, S. V. Meille, A. Mele, G. B. Appetecchi, and S. Passerini, "Pyrrolidinium-Based Ionic Liquids Doped with Lithium Salts: How Does Li⁺ Coordination Affect Its Diffusivity?," *J. Phys. Chem. B*, vol. 118, no. 47, pp. 13679–13688, 2014.
- ²⁴ L. Aguilera, J. Völkner, A. Labrador, and A. Matic, "The effect of lithium salt doping on the nanostructure of ionic liquids," *Phys. Chem. Chem. Phys.*, vol. 17, no. 40, pp. 27082–27087, 2015.

- ²⁵ T. Méndez-Morales, J. Carrete, O. Cabeza, O. Russina, A. Triolo, L. J. Gallego, and L. M. Varela, "Solvation of lithium salts in protic ionic liquids: a molecular dynamics study," *J. Phys. Chem. B*, vol. 118, pp. 761–770, 2014.
- ²⁶ O. Russina, R. Caminiti, T. Méndez-Morales, J. Carrete, O. Cabeza, L. J. Gallego, L. M. Varela, and A. Triolo, "How does lithium nitrate dissolve in a protic ionic liquid?," *J. Mol. Liq.*, vol. 205, no. 0, pp. 16 – 21, 2015.
- ²⁷ L. M. Varela, T. Méndez-Morales, J. Carrete, V. Gómez-González, B. Docampo-Álvarez, L. J. Gallego, O. Cabeza, and O. Russina, "Solvation of molecular cosolvents and inorganic salts in ionic liquids: a review of molecular dynamics simulations," *J. Mol. Liq.*, vol. 210, pp. 178–188, 2015.
- ²⁸ L. M. Varela, J. Carrete, M. García, J. R. Rodríguez, L. J. Gallego, M. Turmine, and O. Cabeza, "Pseudolattice theory of ionic liquids," in *Ionic liquids: theory, properties, new approaches* (A. Kokorin, ed.), InTech, 2011.
- ²⁹ S. A. Kislenko, I. S. Samoylov, and R. H. Amirov, "Molecular dynamics simulation of the electrochemical interface between a graphite surface and the ionic liquid [BMIM][PF₆]," *Phys. Chem. Chem. Phys.*, vol. 11, no. 27, pp. 5584–5590, 2009.
- ³⁰ M. V. Fedorov and R. M. Lynden-Bell, "Probing the neutral graphene–ionic liquid interface: insights from molecular dynamics simulations," *Phys. Chem. Chem. Phys.*, vol. 14, pp. 2552–2556, 2012.
- ³¹ R. M. Lynden-Bell, A. I. Frolov, and M. V. Fedorov, "Electrode screening by ionic liquids," *Phys. Chem. Chem. Phys.*, vol. 14, no. 8, pp. 2693–2701, 2012.
- ³² C. Pinilla, M. G. Del Pópolo, R. M. Lynden-Bell, and J. Kohanoff, "Structure and dynamics of a confined ionic liquid. topics of rel-

- evance to dye-sensitized solar cells,” *J. Phys. Chem. B*, vol. 109, no. 38, pp. 17922–17927, 2005.
- ³³ A. A. Kornyshev, “Double-layer in ionic liquids: Paradigm change?,” *J. Phys. Chem. B*, vol. 111, no. 20, pp. 5545–5557, 2007.
- ³⁴ M. V. Fedorov and A. A. Kornyshev, “Towards understanding the structure and capacitance of electrical double layer in ionic liquids,” *Electrochim. Acta*, vol. 111, no. 23, pp. 6835–6840, 2008.
- ³⁵ S. Maolin, Z. Fuchun, W. Guozhong, F. Haiping, W. Chunlei, C. Shimou, Z. Yi, and H. Jun, “Ordering layers of [BMIM][PF₆] ionic liquid on graphite surfaces: Molecular dynamics simulation,” *J. Chem. Phys.*, vol. 128, no. 13, p. 134504, 2008.
- ³⁶ G. Feng, J. S. Zhang, and R. Qiao, “Microstructure and capacitance of the electrical double layers at the interface of ionic liquids and planar electrodes,” *J. Phys. Chem. C*, vol. 113, no. 11, pp. 4549–4559, 2009.
- ³⁷ S. A. Kislenko, I. S. Samoylov, and R. H. Amirov, “Molecular dynamics simulation of the electrochemical interface between a graphite surface and the ionic liquid [BMIM][PF₆],” *Phys. Chem. Chem. Phys.*, vol. 11, no. 27, pp. 5584–5590, 2009.
- ³⁸ S. Wang, S. Li, Z. Cao, and T. Yan, “Molecular Dynamic Simulations of Ionic Liquids at Graphite Surface,” *J. Phys. Chem. C*, vol. 114, no. 2, pp. 990–995, 2010.
- ³⁹ Q. Dou, M. L. Sha, H. Y. Fu, and G. Z. Wu, “Molecular dynamics simulation of the interfacial structure of [Cnmim][PF₆] adsorbed on a graphite surface: effects of temperature and alkyl chain length,” *J. Phys.: Condens. Matter*, vol. 23, no. 17, pp. 175001(1)–175001(8), 2011.
- ⁴⁰ R. S. Payal and S. Balasubramanian, “Orientational ordering of ionic liquids near a charged mica surface,” *Chem. Phys. Chem.*, vol. 13, no. 7, pp. 1764–1771, 2012.

- ⁴¹ M. V. Fedorov and A. A. Kornyshev, "Ionic liquids at electrified interfaces," *Chem. Rev.*, vol. 114, no. 5, pp. 2978–3036, 2014.
- ⁴² V. Ivaništšev, S. O'Connor, and M. V. Fedorov, "Poly(a)morphic portrait of the electrical double layer in ionic liquids," *Electrochem. Commun.*, vol. 48, pp. 61–64, 2014.
- ⁴³ V. Ivaništšev, K. Kirchner, T. Kirchner, and M. V. Fedorov, "Restructuring of the electrical double layer in ionic liquids upon charging," *J. Phys.: Condens. Matter*, vol. 27, no. 10, p. 102101, 2015.
- ⁴⁴ A. A. Kornyshev and R. Qiao, "Three-dimensional double layers," *J. Phys. Chem. C*, vol. 118, no. 32, pp. 18285–18290, 2014.
- ⁴⁵ O. Borodin, G. D. Smith, and W. Henderson, "Li⁺ Cation Environment, Transport, and Mechanical Properties of the LiTFSI Doped N-Methyl-N-alkylpyrrolidinium+TFSI[−] Ionic Liquids," *J. Phys. Chem. B*, vol. 110, no. 34, pp. 16879–16886, 2006.
- ⁴⁶ T. Méndez-Morales, J. Carrete, S. Bouzón-Capelo, M. Pérez-Rodríguez, O. Cabeza, L. J. Gallego, and L. M. Varela, "MD Simulations of the Formation of Stable Clusters in Mixtures of Alkaline Salts and Imidazolium-Based Ionic Liquids," *J. Phys. Chem. B*, vol. 117, no. 11, pp. 3207–3220, 2013.
- ⁴⁷ J. B. Haskins, W. R. Bennett, J. J. Wu, D. M. Hernández, O. Borodin, J. D. Monk, C. W. Bauschlicher, and J. W. Lawson, "Computational and experimental investigation of li-doped ionic liquid electrolytes: [pyr14][TFSI], [pyr13][FSI], and [EMIM][BF₄]," *J. Phys. Chem. B*, vol. 118, no. 38, pp. 11295–11309, 2014.
- ⁴⁸ C. W. Bauschlicher, J. B. Haskins, E. W. Bucholz, J. W. Lawson, and O. Borodin, "Structure and Energetics of Li⁺–(BF₄[−])_n, Li⁺–(FSI[−])_n, and Li⁺–(TFSI[−])_n: Ab Initio and Polarizable Force Field Approaches," *J. Phys. Chem. B*, vol. 118, no. 36, pp. 10785–10794, 2014.

- ⁴⁹ Z. Li, O. Borodin, G. D. Smith, and D. Bedrov, "Effect of Organic Solvents on Li^+ Ion Solvation and Transport in Ionic Liquid Electrolytes: A Molecular Dynamics Simulation Study," *J. Phys. Chem. B*, vol. 119, no. 7, pp. 3085–3096, 2015.
- ⁵⁰ T. Méndez-Morales, J. Carrete, J. R. Rodríguez, Ó. Cabeza, L. J. Gallego, O. Russina, and L. M. Varela, "Nanostructure of mixtures of protic ionic liquids and lithium salts: effect of alkyl chain length," *Phys. Chem. Chem. Phys.*, vol. 17, no. 7, pp. 5298–5307, 2015.
- ⁵¹ T. Méndez-Morales, J. Carrete, M. Pérez-Rodríguez, O. Cabeza, L. J. Gallego, R. M. Lynden-Bell, and L. M. Varela, "Molecular dynamics simulations of the structure of the graphene-ionic liquid/alkali salt mixtures interface," *Phys. Chem. Chem. Phys.*, vol. 16, pp. 13271–13278, 2014.
- ⁵² V. Ivaništšev, T. Méndez-Morales, R. M. Lynden-Bell, O. Cabeza, L. J. Gallego, L. M. Varela, and M. V. Fedorov, "Molecular origin of high free energy barriers for alkali metal ion transfer through ionic liquid–graphene electrode interfaces," *Phys. Chem. Chem. Phys.*, vol. 18, no. 2, pp. 1302–1310, 2016.
- ⁵³ G. T. Cheek, W. E. O'Grady, S. Z. El Abedin, E. M. Moustafa, and F. Endres, "Studies on the electrodeposition of magnesium in ionic liquids," *J. Electrochem. Soc.*, vol. 155, no. 1, pp. D91–D95, 2008.
- ⁵⁴ G. A. Giffin, A. Moretti, S. Jeong, and S. Passerini, "Complex Nature of Ionic Coordination in Magnesium Ionic Liquid-Based Electrolytes: Solvates with Mobile Mg^{2+} Cations," *J. Phys. Chem. C*, vol. 118, no. 19, pp. 9966–9973, 2014.
- ⁵⁵ G. Vardar, A. E. S. Sleightholme, J. Naruse, H. Hiramatsu, D. J. Siegel, and C. W. Monroe, "Electrochemistry of Magnesium Electrolytes in Ionic Liquids for Secondary Batteries," *ACS Appl. Mater. Interfaces.*, vol. 6, no. 20, pp. 18033–18039, 2014.
- ⁵⁶ S. Saha, T. Taguchi, N. Tachikawa, K. Yoshii, and Y. Katayama, "Electrochemical behavior of cadmium in 1-

butyl-1-methylpyrrolidinium bis(trifluoromethylsulfonyl)amide room-temperature ionic liquid,” *Electrochim. Acta*, vol. 183, pp. 42 – 48, 2015.

⁵⁷ R. Atkin and G. G. Warr, “The smallest amphiphiles: Nanostructure in protic room-temperature ionic liquids with short alkyl groups,” *J. Phys. Chem. B*, vol. 112, no. 14, pp. 4164–4166, 2008.

⁵⁸ R. Hayes, S. Imberti, G. G. Warr, and R. Atkin, “Pronounced sponge-like nanostructure in propylammonium nitrate,” *Phys. Chem. Chem. Phys.*, vol. 13, no. 30, pp. 13544–13551, 2011.

⁵⁹ D. R. MacFarlane, N. Tachikawa, M. Forsyth, J. M. Pringle, P. C. Howlett, G. D. Elliott, J. H. Davis, M. Watanabe, P. Simon, and C. A. Angell, “Energy applications of ionic liquids,” *Energy Environ. Sci.*, vol. 7, no. 1, pp. 232–250, 2014.

⁶⁰ T. Vogl, C. Vaalma, D. Buchholz, M. Secchiaroli, R. Marassi, S. Passerini, and A. Balducci, “The use of protic ionic liquids with cathodes for sodium-ion batteries,” *J. Mater. Chem. A*, vol. 4, no. 27, pp. 10472–10478, 2016.

⁶¹ B. Dilasari, Y. Jung, and K. Kwon, “Comparative study of corrosion behavior of metals in protic and aprotic ionic liquids,” *Electrochem. Commun.*, vol. 73, pp. 20–23, 2016.

⁶² T. Vogl, S. Passerini, and A. Balducci, “The impact of mixtures of protic ionic liquids on the operative temperature range of use of battery systems,” *Electrochem. Commun.*, vol. 78, pp. 47–50, 2017.

⁶³ S. Z. El Abedin, E. Moustafa, R. Hempelmann, H. Natter, and F. Endres, “Additive free electrodeposition of nanocrystalline aluminium in a water and air stable ionic liquid,” *Electrochem. Commun.*, vol. 7, no. 11, pp. 1111–1116, 2005.

⁶⁴ S. Z. El Abedin, P. Giridhar, P. Schwab, and F. Endres, “Electrodeposition of nanocrystalline aluminium from a chloroaluminate ionic

- liquid,” *Electrochem. Commun.*, vol. 12, no. 8, pp. 1084–1086, 2010.
- ⁶⁵ Q. Liu, S. Z. El Abedin, and F. Endres, “Electroplating of mild steel by aluminium in a first generation ionic liquid: A green alternative to commercial Al-plating in organic solvents,” *Surf. Coat. Technol.*, vol. 201, no. 3, pp. 1352–1356, 2006.
- ⁶⁶ X. Liu, F. Zhou, Y. Liang, and W. Liu, “Tribological performance of phosphonium based ionic liquids for an aluminum-on-steel system and opinions on lubrication mechanism,” *Wear*, vol. 261, no. 10, pp. 1174–1179, 2006.
- ⁶⁷ Z. Mu, F. Zhou, S. Zhang, Y. Liang, and W. Liu, “Effect of the functional groups in ionic liquid molecules on the friction and wear behavior of aluminum alloy in lubricated aluminum-on-steel contact,” *Tribol. Int.*, vol. 38, no. 8, pp. 725–731, 2005.
- ⁶⁸ J. Sun, R. C. Remsing, Y. Zhang, Z. Sun, A. Ruzsinszky, H. Peng, Z. Yang, A. Paul, U. Waghmare, X. Wu, *et al.*, “SCAN: An Efficient Density Functional Yielding Accurate Structures and Energies of Diversely-Bonded Materials,” *arXiv preprint arXiv:1511.01089*, 2015.
- ⁶⁹ M.-C. Lin, M. Gong, B. Lu, Y. Wu, D.-Y. Wang, M. Guan, M. Angell, C. Chen, J. Yang, B.-J. Hwang, *et al.*, “An ultrafast rechargeable aluminium-ion battery,” *Nature*, vol. 520, no. 7547, p. 324, 2015.
- ⁷⁰ R. A. Marcus, “On the theory of oxidation-reduction reactions involving electron transfer. I,” *J. Chem. Phys.*, vol. 24, no. 5, pp. 966–978, 1956.
- ⁷¹ R. M. Lynden-Bell, “Can Marcus theory be applied to redox processes in ionic liquids? A comparative simulation study of dimethylimidazolium liquids and acetonitrile,” *The J. Phys. Chem. B*, vol. 111, no. 36, pp. 10800–10806, 2007.

- ⁷² R. M. Lynden-Bell, “Does Marcus theory apply to redox processes in ionic liquids? A simulation study,” *Electrochem. Comm.*, vol. 9, no. 8, pp. 1857–1861, 2007.
- ⁷³ Z. Li, G. Jeanmairet, T. Méndez-Morales, M. Burbano, M. Haelele, and M. Salanne, “Confinement effects on an electron transfer reaction in nanoporous carbon electrodes,” *J. Phys. Chem. Lett.*, vol. 8, no. 9, pp. 1925–1931, 2017.
- ⁷⁴ F. Gao, H. Xiao, X. Zu, M. Posselt, and W. J. Weber, “Defect-enhanced charge transfer by ion-solid interactions in SiC using large-scale ab initio molecular dynamics simulations,” *Phys. Rev. Lett.*, vol. 103, no. 2, pp. 027405–027408, 2009.
- ⁷⁵ V. Chevrier, J. Zwanziger, and J. Dahn, “First principles study of Li–Si crystalline phases: charge transfer, electronic structure, and lattice vibrations,” *J. Alloys Compd.*, vol. 496, no. 1, pp. 25–36, 2010.
- ⁷⁶ A. Kokalj, “On the HSAB based estimate of charge transfer between adsorbates and metal surfaces,” *Chem. Phys.*, vol. 393, no. 1, pp. 1–12, 2012.
- ⁷⁷ M. Shukla, N. Srivastava, and S. Saha, “Investigation of ground state charge transfer complex between paracetamol and p-chloranil through DFT and UV–visible studies,” *J. Mol. Struct.*, vol. 1021, pp. 153–157, 2012.
- ⁷⁸ O. Leenaerts, B. Partoens, and F. Peeters, “Paramagnetic adsorbates on graphene: a charge transfer analysis,” *Appl. Phys. Lett.*, vol. 92, no. 24, pp. 243125–243127, 2008.
- ⁷⁹ H. Valencia, M. Kohyama, S. Tanaka, and H. Matsumoto, “Ab initio study of EMIM-BF₄ crystal interaction with a Li (100) surface as a model for ionic liquid/Li interfaces in Li-ion batteries,” *J. Chem. Phys.*, vol. 131, pp. 244705–244715, 2009.

- ⁸⁰ F. Buchner, K. Forster-Tonigold, B. Uhl, D. Alwast, N. Wagner, H. Farkhondeh, A. Groß, and R. J. Behm, "Toward the microscopic identification of anions and cations at the ionic liquid/Ag(111) interface: a combined experimental and theoretical investigation," *ACS Nano*, vol. 7, pp. 7773–7784, 2013.
- ⁸¹ F. Buchner, K. Forster-Tonigold, M. Bozorgchenani, A. Gross, and R. J. Behm, "Interaction of a self-assembled ionic liquid layer with graphite(0001): a combined experimental and theoretical study," *J. Phys. Chem. Lett.*, vol. 7, pp. 226–233, 2016.
- ⁸² V. Koch, L. Dominey, C. Nanjundiah, and M. J. Ondrechen, "The intrinsic anodic stability of several anions comprising solvent-free ionic liquids," *J. Electrochem. Soc.*, vol. 143, pp. 798–803, 1996.
- ⁸³ M. Ue, A. Murakami, and S. Nakamura, "A convenient method to estimate ion size for electrolyte materials design," *J. Electrochem. Soc.*, vol. 149, pp. A1385–A1388, 2002.
- ⁸⁴ J. M. Vollmer, L. A. Curtiss, D. R. Vissers, and K. Amine, "Reduction mechanisms of ethylene, propylene, and vinylene carbonates: a quantum chemical study," *J. Electrochem. Soc.*, vol. 151, pp. A178–A183, 2004.
- ⁸⁵ A. Budi, A. Basile, G. Opletal, A. F. Hollenkamp, A. S. Best, R. J. Rees, A. I. Bhatt, A. P. O'Mullane, and S. P. Russo, "Study of the initial stage of solid electrolyte interphase formation upon chemical reaction of lithium metal and n-methyl-n-propyl-pyrrolidinium-bis(fluorosulfonyl)imide," *J. Phys. Chem. C*, vol. 116, pp. 19789–19797, 2012.
- ⁸⁶ L. E. Camacho-Forero, T. W. Smith, S. Bertolini, and P. B. Balbuena, "Reactivity at the lithium-metal anode surface of lithium-sulfur batteries," *J. Phys. Chem. C*, vol. 119, pp. 26828–26839, 2015.
- ⁸⁷ K. Sodeyama, Y. Yamada, K. Aikawa, A. Yamada, and Y. Tateyama, "Sacrificial anion reduction mechanism for electrochemical sta-

- bility improvement in highly concentrated Li-salt electrolyte,” *J. Phys. Chem. C*, vol. 118, pp. 14091–14097, 2014.
- ⁸⁸ D. M. Piper, T. Evans, K. Leung, T. Watkins, J. Olson, S. C. Kim, S. S. Han, V. Bhat, K. W. Oh, D. A. Buttry, and S.-H. Lee, “Stable silicon-ionic liquid interface for next-generation lithium-ion batteries,” *Nat. Commun.*, vol. 6, pp. 6230–6239, 2015.
- ⁸⁹ T. Welton, “Room-temperature ionic liquids. Solvents for synthesis and catalysis,” *Chem. Rev.*, vol. 99, no. 8, pp. 2071–2084, 1999.
- ⁹⁰ N. V. Plechkova and K. R. Seddon, *Ionic Liquids: “Designer” Solvents for Green Chemistry*, pp. 103–130. John Wiley & Sons, Inc., 2007.
- ⁹¹ P. Wasserscheid and M. Keim, “Ionic Liquids—New “Solutions” for Transition Metal Catalysis,” *Angew. Chem. Int. Ed. Engl.*, vol. 39, no. 21, pp. 3772–3789, 2000.
- ⁹² P. Wasserscheid and T. Welton, *Ionic liquids in synthesis*. Wiley Online Library, 2003.
- ⁹³ M. Freemantle, *An Introduction to Ionic Liquids*. RSC Publishing, 2009.
- ⁹⁴ M. T. Garcia, N. Gathergood, and P. J. Scammells, “Biodegradable ionic liquids Part II. Effect of the anion and toxicology,” *Green Chem.*, vol. 7, no. 1, pp. 9–14, 2005.
- ⁹⁵ D. R. MacFarlane, M. Forsyth, P. C. Howlett, J. M. Pringle, J. Sun, G. Annat, W. Neil, and E. I. Izgorodina, “Ionic liquids in electrochemical devices and processes: managing interfacial electrochemistry,” *Acc. Chem. Res.*, vol. 40, no. 11, pp. 1165–1173, 2007.
- ⁹⁶ M. Armand, F. Endres, D. R. MacFarlane, H. Ohno, and B. Scrosati, “Ionic-liquid materials for the electrochemical challenges of the future,” *Nat. Mater.*, vol. 8, pp. 621–629, 2009.

- ⁹⁷ X. Lu, G. Burrell, F. Separovic, and C. Zhao, "Electrochemistry of Room Temperature Protic Ionic Liquids: A Critical Assessment for Use as Electrolytes in Electrochemical Applications," *J. Phys. Chem. B.*, vol. 116, no. 30, pp. 9160–9170, 2012.
- ⁹⁸ T. Yim, C. Y. Choi, J. Mun, S. M. Oh, and Y. G. Kim, "Synthesis and properties of acyclic ammonium-based ionic liquids with allyl substituents as electrolytes," *Molecules*, vol. 14, no. 5, pp. 1840–1851, 2009.
- ⁹⁹ J. N. Canongia-Lopes, M. F. Costa-Gomes, and A. A. H. Pádua, "Nonpolar, polar, and associating solutes in ionic liquids," *J. Phys. Chem. B*, vol. 110, no. 34, pp. 16816–16818, 2006.
- ¹⁰⁰ A. Triolo, O. Russina, H.-J. Bleif, and E. Di Cola, "Nanoscale segregation in room temperature ionic liquids," *J. Phys. Chem. B*, vol. 111, no. 18, pp. 4641–4644, 2007.
- ¹⁰¹ M. Hirao, H. Sugimoto, and H. Ohno, "Preparation of Novel Room-Temperature Molten Salts by Neutralization of Amines," *J. Electrochem. Soc.*, vol. 147, no. 11, pp. 4168–4172, 2000.
- ¹⁰² M. Yoshizawa, W. Ogihara, and H. Ohno, "Design of new ionic liquids by neutralization of imidazole derivatives with imide-type acids," *Electrochem. Solid State Lett.*, vol. 4, no. 6, pp. E25–E27, 2001.
- ¹⁰³ A. W. K. Fumino and R. Ludwig, "Hydrogen bonding in protic ionic liquids: Reminiscent of water," *Angew. Chem. Int. Ed.*, vol. 48, no. 17, pp. 3184–3186, 2009.
- ¹⁰⁴ R. Hayes, S. Imberti, G. G. Warr, and R. Atkin, "The nature of hydrogen bonding in protic ionic liquids," *Angew. Chem. Int. Ed.*, vol. 52, no. 17, pp. 4623–4627, 2013.
- ¹⁰⁵ E. J. Maginn, "Molecular simulation of ionic liquids: current status and future opportunities," *J. Phys. Condens. Matter*, vol. 21, no. 37, p. 373101, 2009.

- ¹⁰⁶ K. Dong, X. Liu, H. Dong, X. Zhang, and S. Zhang, “Multiscale studies on ionic liquids,” *Chemicalm. Rev.*, vol. 117, no. 10, pp. 6636–6695, 2017.
- ¹⁰⁷ B. Hess, C. Kutzner, D. V. D. Spoel, and E. Lindahl, “Gromacs 4: Algorithms for highly efficient, load-balanced, and scalable molecular simulation,” *J. Chem. Theory Comput.*, vol. 4, no. 3, pp. 435–447, 2008.
- ¹⁰⁸ M. J. Abraham, T. Murtola, R. Schulz, S. Páll, J. C. Smith, B. Hess, and E. Lindahl, “GROMACS: High performance molecular simulations through multi-level parallelism from laptops to supercomputers,” *SoftwareX*, vol. 1, pp. 19–25, 2015.
- ¹⁰⁹ L. Martínez, R. Andrade, E. G. Birgin, and J. M. Martínez, “Packmol: A package for building initial configurations for molecular dynamics simulations,” *J. Comput. Chem.*, vol. 30, no. 13, pp. 2157–2164, 2009.
- ¹¹⁰ L. Verlet, “Computer “experiments” on classical fluids. I. Thermodynamical properties of Lennard-Jones molecules,” *Phys. Rev.*, vol. 159, no. 1, p. 98, 1967.
- ¹¹¹ W. L. Jorgensen, “Optimized intermolecular potential functions for liquid alcohols,” *J. Phys. Chem.*, vol. 90, no. 7, pp. 1276–1284, 1986.
- ¹¹² J. N. C. Lopes and A. A. Pádua, “CL&P: A generic and systematic force field for ionic liquids modeling,” *Theor. Chem. Acc.*, vol. 131, no. 3, p. 1129, 2012.
- ¹¹³ K. Vanommeslaeghe, E. Hatcher, C. Acharya, S. Kundu, S. Zhong, J. Shim, E. Darian, O. Guvench, P. Lopes, I. Vorobyov, *et al.*, “CHARMM general force field: A force field for drug-like molecules compatible with the CHARMM all-atom additive biological force fields,” *J. Comput. Chem.*, vol. 31, no. 4, pp. 671–690, 2010.
- ¹¹⁴ W. F. van Gunsteren, X. Daura, and A. E. Mark, “Gromos force field,” *Encyclopedia of computational chemistry*, vol. 2, 2002.

- ¹¹⁵ J. Wang, R. M. Wolf, J. W. Caldwell, P. A. Kollman, and D. A. Case, "Development and testing of a general amber force field," *J. Comput. Chem.*, vol. 25, no. 9, pp. 1157–1174, 2004.
- ¹¹⁶ T. Darden, D. York, and L. Pedersen, "Particle mesh ewald: An $n \log(n)$ method for ewald sums in large systems," *J. Chem. Phys.*, vol. 98, no. 12, pp. 10089–10094, 1993.
- ¹¹⁷ I. Yeh and M. L. Berkowitz, "Ewald summation for systems with slab geometry," *J. Chem. Phys.*, vol. 111, no. 7, pp. 3155–3162, 1999.
- ¹¹⁸ R. M. Martin, *Electronic structure: basic theory and practical methods*. Cambridge university press, 2004.
- ¹¹⁹ W. Kohn, "Nobel Lecture: Electronic structure of matter—wave functions and density functionals," *Rev. Mod. Phys.*, vol. 71, no. 5, p. 1253, 1999.
- ¹²⁰ N. Mardirossian and M. Head-Gordon, "Thirty years of density functional theory in computational chemistry: an overview and extensive assessment of 200 density functionals," *Mol. Phys.*, vol. 115, no. 19, pp. 2315–2372, 2017.
- ¹²¹ J. P. Perdew and A. Zunger, "Self-interaction correction to density-functional approximations for many-electron systems," *Phys. Rev. B*, vol. 23, no. 10, p. 5048, 1981.
- ¹²² J. P. Perdew, K. Burke, and M. Ernzerhof, "Generalized gradient approximation made simple," *Phys. Rev. Lett.*, vol. 77, no. 18, p. 3865, 1996.
- ¹²³ A. D. Becke, "A new mixing of Hartree–Fock and local density-functional theories," *J. Chem. Phys.*, vol. 98, no. 2, pp. 1372–1377, 1993.
- ¹²⁴ C. Lee, W. Yang, and R. G. Parr, "Development of the Colle-Salvetti correlation-energy formula into a functional of the electron density," *Phys. Rev. B*, vol. 37, no. 2, p. 785, 1988.

- ¹²⁵ M. Valiev, E. J. Bylaska, N. Govind, K. Kowalski, T. P. Straatsma, H. J. Van Dam, D. Wang, J. Nieplocha, E. Apra, T. L. Windus, *et al.*, “NWChem: a comprehensive and scalable open-source solution for large scale molecular simulations,” *Comput. Phys. Commun.*, vol. 181, no. 9, pp. 1477–1489, 2010.
- ¹²⁶ M. J. Frisch, G. W. Trucks, H. B. Schlegel, G. E. Scuseria, M. A. Robb, J. R. Cheeseman, G. Scalmani, V. Barone, G. A. Petersson, H. Nakatsuji, X. Li, M. Caricato, A. V. Marenich, J. Bloino, B. G. Janesko, R. Gomperts, B. Mennucci, H. P. Hratchian, J. V. Ortiz, A. F. Izmaylov, J. L. Sonnenberg, D. Williams-Young, F. Ding, F. Lipparini, F. Egidi, J. Goings, B. Peng, A. Petrone, T. Henderson, D. Ranasinghe, V. G. Zakrzewski, J. Gao, N. Rega, G. Zheng, W. Liang, M. Hada, M. Ehara, K. Toyota, R. Fukuda, J. Hasegawa, M. Ishida, T. Nakajima, Y. Honda, O. Kitao, H. Nakai, T. Vreven, K. Throssell, J. A. Montgomery, Jr., J. E. Peralta, F. Ogliaro, M. J. Bearpark, J. J. Heyd, E. N. Brothers, K. N. Kudin, V. N. Staroverov, T. A. Keith, R. Kobayashi, J. Normand, K. Raghavachari, A. P. Rendell, J. C. Burant, S. S. Iyengar, J. Tomasi, M. Cossi, J. M. Millam, M. Klene, C. Adamo, R. Cammi, J. W. Ochterski, R. L. Martin, K. Morokuma, O. Farkas, J. B. Foresman, and D. J. Fox, “Gaussian 16 Revision A.03,” 2016. Gaussian Inc. Wallingford CT.
- ¹²⁷ G. Kresse and J. Furhmüller, “Software VASP, Vienna (1999); G. Kresse, J. Hafner,” *Phys. Rev. B*, vol. 47, p. R558, 1993.
- ¹²⁸ G. Kresse and J. Furthmüller, “Efficient iterative schemes for ab initio total-energy calculations using a plane-wave basis set,” *Phys. Rev. B*, vol. 54, no. 16, p. 11169, 1996.
- ¹²⁹ G. Kresse and J. Furthmüller, “Efficiency of ab-initio total energy calculations for metals and semiconductors using a plane-wave basis set,” *Comput. Mater. Sci.*, vol. 6, no. 1, pp. 15–50, 1996.

- ¹³⁰ G. Kresse and D. Joubert, "From ultrasoft pseudopotentials to the projector augmented-wave method," *Phys. Rev. B*, vol. 59, no. 3, p. 1758, 1999.
- ¹³¹ V. Gómez-González, B. Docampo-Álvarez, O. Cabeza, M. V. Fedorov, R. M. Lynden-Bell, L. J. Gallego, and L. M. Varela, "Molecular dynamics simulations of the structure and single-particle dynamics of mixtures of divalent salts and ionic liquids," *J. Chem. Phys.*, vol. 143, no. 12, p. 124507, 2015.
- ¹³² R. D. Rogers and K. R. Seddon, "Ionic liquids—solvents of the future?," *Science*, vol. 302, no. 5646, pp. 792–793, 2003.
- ¹³³ J. Dupont, R. F. de Souza, and P. A. Z. Suarez, "Ionic liquid (molten salt) phase organometallic catalysis," *Chem. Rev.*, vol. 102, no. 10, pp. 3667–3692, 2002.
- ¹³⁴ A. P. Abbott and K. J. McKenzie, "Application of ionic liquids to the electrodeposition of metals," *Phys. Chem. Chem. Phys.*, vol. 8, pp. 4265–4279, 2006.
- ¹³⁵ A. Chaumont, E. Engler, and G. Wipff, "Uranyl and strontium salt solvation in room-temperature ionic liquids. a molecular dynamics investigation," *Inorganic Chemistry*, vol. 42, no. 17, pp. 5348–5356, 2003.
- ¹³⁶ A. Chaumont and G. Wipff, "Solvation of uranyl-CMPO complexes in dry vs. humid forms of the [BMI][PF₆] ionic liquid. A molecular dynamics study," *Phys. Chem. Chem. Phys.*, vol. 8, pp. 494–502, 2006.
- ¹³⁷ C. Gaillard, A. Chaumont, I. Billard, C. Hennig, A. Ouadi, and G. Wipff, "Uranyl Coordination in Ionic Liquids: The Competition between Ionic Liquid Anions, Uranyl Counterions, and Cl⁻ Anions Investigated by Extended X-ray Absorption Fine Structure and UV–Visible Spectroscopies and Molecular Dynamics Simulations," *Inorganic Chemistry*, vol. 46, no. 12, pp. 4815–4826, 2007.

- ¹³⁸ A. Chaumont, O. Klimchuk, C. Gaillard, I. Billard, A. Ouadi, C. Hennig, and G. Wipff, "Perrhenate Complexation by Uranyl in Traditional Solvents and in Ionic Liquids: A Joint Molecular Dynamics/Spectroscopic Study," *J. Phys. Chem. B*, vol. 116, no. 10, pp. 3205–3219, 2012.
- ¹³⁹ D. V. D. Spoel, E. Lindahl, B. Hess, A. R. V. Buuren, E. Apol, P. J. Meulenhoff, D. P. Tieleman, A. L. T. M. Sijbers, K. A. Feenstra, R. V. Drunen, and H. J. C. Berendsen, *Gromacs User Manual version 4.6.7*. <http://www.Gromacs.org>, 2014.
- ¹⁴⁰ W. L. Jorgensen and J. D. Madura, "Quantum and statistical mechanical studies of liquids. 25. solvation and conformation of methanol in water," *J. Am. Chem. Soc.*, vol. 105, no. 6, pp. 1407–1413, 1983.
- ¹⁴¹ Y. Umebayashi, W.-L. Chung, T. Mitsugi, S. Fukuda, M. Takeuchi, K. Fujii, T. Takamuku, R. Kanzaki, and S. Ishiguro, "Liquid Structure and the Ion-Ion Interactions of Ethylammonium Nitrate Ionic Liquid Studied by Large Angle X-Ray Scattering and Molecular Dynamics Simulations," *J. Comput. Chem. Jpn.*, vol. 7, no. 4, pp. 125–134, 2008.
- ¹⁴² J. Choe, K. Kim, and S. Chang, "Computer simulations on molecular recognition of alkylamines by ester derivatives of p-tert-butylcalix[6]arene," *Bull. Korean Chem. Soc.*, vol. 21, no. 2, pp. 200–206, 2000.
- ¹⁴³ J. Aqvist, "Ion-water interaction potentials derived from free energy perturbation simulations," *J. Phys. Chem.*, vol. 94, no. 21, pp. 8021–8024, 1990.
- ¹⁴⁴ S. V. Sambasivarao and O. Acevedo, "Development of OPLS-AA Force Field Parameters for 68 Unique Ionic Liquids," *J. Chem. Theory Comput.*, vol. 5, no. 4, pp. 1038–1050, 2009.

- ¹⁴⁵ B. Hess, H. Bekker, H. J. C. Berendsen, and J. G. E. M. Fraaije, "Lincs: A linear constraint solver for molecular simulations," *J. Comp. Chem.*, vol. 18, no. 12, pp. 1463–1472, 1997.
- ¹⁴⁶ B. Hess, "P-lincs: A parallel linear constraint solver for molecular simulation," *J. Chem. Theory Comp.*, vol. 4, no. 1, pp. 116–122, 2007.
- ¹⁴⁷ G. Bussi, D. Donadio, and M. Parrinello, "Canonical sampling through velocity rescaling," *J. Chem. Phys.*, vol. 126, no. 1, pp. 014101(1)–014101(7), 2007.
- ¹⁴⁸ M. Parrinello and A. Rahman, "Polymorphic transitions in single crystals: A new molecular dynamics method," *J. Appl. Phys.*, vol. 52, no. 12, pp. 7182–7190, 1981.
- ¹⁴⁹ S. Feng and G. A. Voth, "Molecular dynamics simulations of imidazolium-based ionic liquid/water mixtures: Alkyl side chain length and anion effects," *Fluid Phase Equilib.*, vol. 294, no. 1–2, pp. 148–156, 2010.
- ¹⁵⁰ G. Raabe and J. Köhler, "Thermodynamical and structural properties of binary mixtures of imidazolium chloride ionic liquids and alcohols from molecular simulation," *J. Chem. Phys.*, vol. 129, no. 14, pp. 144503(1)–144503(8), 2008.
- ¹⁵¹ Y. Marcus, G. Hefter, and T.-S. Pang, "Ionic partial molar volumes in non-aqueous solvents," *J. Chem. Soc., Faraday Trans.*, vol. 90, pp. 1899–1903, 1994.
- ¹⁵² Y. Marcus, "The Standard Partial Molar Volumes of Ions in Solution. Part 2. The Volumes in Two Binary Solvent Mixtures with No Preferential Solvation," *J. Solution Chem.*, vol. 33, no. 5, pp. 549–559, 2004.
- ¹⁵³ Y. Marcus, "The standard partial molar volumes of ions in solution: Part 1. The volumes in single non-aqueous solvents at 298.15 K," *J. Mol. Liq.*, vol. 118, no. 1–3, pp. 3 – 8, 2005.

- ¹⁵⁴ Y. Marcus, "Effect of ions on the structure of water: Structure making and breaking," *Chem. Rev.*, vol. 109, pp. 1346–1370, 2009.
- ¹⁵⁵ Y. Marcus, "The Standard Partial Molar Volumes of Ions in Solution. Part 4. Ionic Volumes in Water at 0–100 °C," *J. Phys. Chem. B*, vol. 113, no. 30, pp. 10285–10291, 2009.
- ¹⁵⁶ Y. Marcus, "Electrostriction in Electrolyte Solutions," *Chem. Rev.*, vol. 111, no. 4, pp. 2761–2783, 2011.
- ¹⁵⁷ Y. Marcus, "The Molar Volumes of Ions in Solution, Part 7. Electrostriction and Hydration Numbers of Aqueous Polyatomic Anions at 25 °C," *J. Phys. Chem. B*, vol. 118, no. 8, pp. 2172–2175, 2014.
- ¹⁵⁸ H. Ohno and K. Furukawa, "Structural analysis of some molten materials by X-ray diffraction. Part 4.-Alkali nitrates RNO_3 ($R = Li, Na, K, Rb, Cs$ and Ag)," *J. Chem. Soc., Faraday Trans. 1*, vol. 74, pp. 297–305, 1978.
- ¹⁵⁹ K. O. Stromme, "On the Crystal Structure of Lithium Nitrate above Room Temperature," *Acta Chem. Scand.*, vol. 24, no. 4, pp. 1479–1481, 1970.
- ¹⁶⁰ M. Ferrario, M. Haughney, I. R. McDonald, and M. L. Klein, "Molecular-dynamics simulation of aqueous mixtures: Methanol, acetone, and ammonia," *J. Chem. Phys.*, vol. 93, no. 7, pp. 5156–5166, 1990.
- ¹⁶¹ R. Gurney, *Ionic processes in solution*. International chemical series, McGraw-Hill, 1953.
- ¹⁶² R. M. Khusnutdinoff and A. V. Mokshin, "Vibrational features of water at the low-density/high-density liquid structural transformations," *Physica A*, vol. 391, no. 9, pp. 2842–2847, 2012.
- ¹⁶³ F. Rull and H. Ohtaki, "Raman spectral studies on ionic interaction in aqueous alkali sulfate solutions," *Spectrochim. Acta*, vol. 53, no. 5, pp. 643–653, 1997.

- ¹⁶⁴ V. Gómez-González, B. Docampo-Álvarez, T. Méndez-Morales, O. Cabeza, V. B. Ivaništšev, M. V. Fedorov, L. J. Gallego, and L. M. Varela, "Molecular dynamics simulation of the structure and interfacial free energy barriers of mixtures of ionic liquids and divalent salts near a graphene wall," *Phys. Chem. Chem. Phys.*, vol. 19, no. 1, pp. 846–853, 2017.
- ¹⁶⁵ M. Salanne, "Simulations of room temperature ionic liquids: from polarizable to coarse-grained force fields," *Physical Chemistry Chemical Physics*, vol. 17, no. 22, pp. 14270–14279, 2015.
- ¹⁶⁶ B. Docampo-Álvarez, V. Gómez-González, H. Montes-Campos, J. M. Otero-Mato, T. Méndez-Morales, O. Cabeza, L. J. Gallego, R. M. Lynden-Bell, V. B. Ivaništšev, M. V. Fedorov, and L. M. Varela, "Molecular dynamics simulation of the behaviour of water in nano-confined ionic liquid–water mixtures," *J. Phys.: Condens. Matter*, vol. 28, no. 46, p. 464001, 2016.
- ¹⁶⁷ B. Rotenberg and M. Salanne, "Structural Transitions at Ionic Liquid Interfaces," *J. Phys. Chem. Lett.*, vol. 6, no. 24, pp. 4978–4985, 2015.
- ¹⁶⁸ K. Kirchner, T. Kirchner, V. Ivaništšev, and M. Fedorov, "Electrical double layer in ionic liquids: Structural transitions from multilayer to monolayer structure at the interface," *Electrochim. Acta*, vol. 110, pp. 762–771, 2013.
- ¹⁶⁹ J. Wallauer, M. Drüscher, B. Huber, and B. Roling, "The Differential Capacitance of Ionic Liquid | Metal Electrode Interfaces – A Critical Comparison of Experimental Results with Theoretical Predictions," *Z. Naturforsch. B*, vol. 68, pp. 1143–1153, 2013.
- ¹⁷⁰ V. Ivaništšev, M. V. Fedorov, and R. M. Lynden-Bell, "Screening of ion–graphene electrode interactions by ionic liquids: the effects of liquid structure," *J. Phys. Chem. C*, vol. 118, no. 11, pp. 5841–5847, 2014.

- ¹⁷¹ J. P. Hansen and I. R. McDonald, *Theory of simple liquids*. Academic press: Oxford, 1986.
- ¹⁷² V. Gómez-González, B. Docampo-Álvarez, J. M. Otero-Mato, O. Cabeza, L. J. Gallego, and L. M. Varela, "Molecular dynamics simulations of the structure of mixtures of protic ionic liquids and monovalent and divalent salts at the electrochemical interface," *Phys. Chem. Chem. Phys.*, vol. 20, no. 18, pp. 12767–12776, 2018.
- ¹⁷³ A. Lahiri, G. Li, M. Olschewski, and F. Endres, "Influence of Polar Organic Solvents in an Ionic Liquid Containing Lithium Bis (fluoro-sulfonyl) amide: Effect on the Cation–Anion Interaction, Lithium Ion Battery Performance, and Solid Electrolyte Interphase," *ACS Appl. Mater. Interfaces*, vol. 8, no. 49, pp. 34143–34150, 2016.
- ¹⁷⁴ R. Ditchfield, W. J. Hehre, and J. A. Pople, "Self-consistent molecular-orbital methods. IX. An extended Gaussian-type basis for molecular-orbital studies of organic molecules," *J. Chem. Phys.*, vol. 54, no. 2, pp. 724–728, 1971.
- ¹⁷⁵ H. Montes-Campos, J. M. Otero-Mato, T. Mendez-Morales, O. Cabeza, L. J. Gallego, A. Ciach, and L. M. Varela, "Two-dimensional pattern formation in ionic liquids confined between graphene walls," *Phys. Chem. Chem. Phys.*, vol. 19, pp. 24505–24512, 2017.
- ¹⁷⁶ R. M. Lynden-Bell, N. A. Atamas, A. Vasilyuk, and C. G. Hanke, "Chemical potentials of water and organic solutes in imidazolium ionic liquids: A simulation study," *Mol. Phys.*, vol. 100, no. 20, pp. 3225–3229, 2002.
- ¹⁷⁷ C. Chipot, B. Maigret, J. L. Rivail, and H. A. Scheraga, "Modeling amino acid side chains. 1. Determination of net atomic charges from ab initio self-consistent-field molecular electrostatic properties," *J. Phys. Chem.*, vol. 96, no. 25, pp. 10276–10284, 1992.
- ¹⁷⁸ V. Gómez-González, B. Docampo-Álvarez, H. Montes-Campos, J. C. Otero, E. López Lago, O. Cabeza, L. J. Gallego, and L. M.

- Varela, "Solvation of Al^{3+} cations in bulk and confined protic ionic liquids: a computational study," *Phys. Chem. Chem. Phys.*, vol. 20, pp. 19071–19081, 2018.
- ¹⁷⁹ M. C. Buzzeo, R. G. Evans, and R. G. Compton, "Non-haloaluminate room-temperature ionic liquids in electrochemistry—a review," *Chem. Phys. Chem.*, vol. 5, no. 8, pp. 1106–1120, 2004.
- ¹⁸⁰ F. Endres and S. Z. E. Abedin, "Air and water stable ionic liquids in physical chemistry," *Phys. Chem. Chem. Phys.*, vol. 8, no. 18, pp. 2101–2116, 2006.
- ¹⁸¹ M. Galiński, A. Lewandowski, and I. Stepniak, "Ionic liquids as electrolytes," *Electrochim. Acta*, vol. 51, pp. 5567–5580, 2006.
- ¹⁸² R. Mohtadi and F. Mizuno, "Magnesium batteries: Current state of the art, issues and future perspectives," *Beilstein J. Nanotechnol.*, vol. 5, p. 1291, 2014.
- ¹⁸³ Y. Orikasa, T. Masese, Y. Koyama, T. Mori, M. Hattori, K. Yamamoto, T. Okado, Z.-D. Huang, T. Minato, C. Tassel, *et al.*, "High energy density rechargeable magnesium battery using earth-abundant and non-toxic elements," *Sci. Rep.*, vol. 4, p. 5622, 2014.
- ¹⁸⁴ G. B. Haxel, J. B. Hedrick, G. J. Orris, P. H. Stauffer, and J. W. Hendley II, "Rare earth elements: critical resources for high technology," tech. rep., 2002.
- ¹⁸⁵ T. M. Faro, G. P. Thim, and M. S. Skaf, "A Lennard-Jones plus Coulomb potential for Al^{3+} ions in aqueous solutions," *J. Chem. Phys.*, vol. 132, no. 11, p. 114509, 2010.
- ¹⁸⁶ A. McLean and G. Chandler, "Contracted Gaussian basis sets for molecular calculations. I. Second row atoms, $Z=11-18$," *J. Chem. Phys.*, vol. 72, no. 10, pp. 5639–5648, 1980.
- ¹⁸⁷ R. Krishnan, J. S. Binkley, R. Seeger, and J. A. Pople, "Self-consistent molecular orbital methods. XX. A basis set for correlated wave functions," *J. Chem. Phys.*, vol. 72, no. 1, pp. 650–654, 1980.

- ¹⁸⁸ B. Docampo-Álvarez, V. Gómez-González, T. Méndez-Morales, J. Carrete, J. R. Rodríguez, O. Cabeza, L. J. Gallego, and L. M. Varela, "Mixtures of protic ionic liquids and molecular cosolvents: A molecular dynamics simulation," *J. Chem. Phys.*, vol. 140, no. 21, p. 214502, 2014.
- ¹⁸⁹ B. Docampo-Álvarez, V. Gómez-González, T. Méndez-Morales, J. R. Rodríguez, E. López-Lago, O. Cabeza, L. J. Gallego, and L. M. Varela, "Molecular dynamics simulations of mixtures of protic and aprotic ionic liquids," *Phys. Chem. Chem. Phys.*, vol. 18, no. 34, pp. 23932–23943, 2016.
- ¹⁹⁰ H. Montes-Campos, J. M. Otero-Mato, T. Méndez-Morales, E. López-Lago, O. Russina, O. Cabeza, L. J. Gallego, and L. M. Varela, "Nanostructured solvation in mixtures of protic ionic liquids and long-chained alcohols," *J. Chem. Phys.*, vol. 146, no. 12, p. 124503, 2017.
- ¹⁹¹ R. D. Shannon, "Revised effective ionic radii and systematic studies of interatomic distances in halides and chalcogenides," *Acta Crystallogr. Sect. A*, vol. 32, no. 5, pp. 751–767, 1976.
- ¹⁹² J. C. Araque, J. J. Hettige, and C. J. Margulis, "Modern room temperature ionic liquids, a simple guide to understanding their structure and how it may relate to dynamics," *J. Phys. Chem. B*, vol. 119, no. 40, pp. 12727–12740, 2015.
- ¹⁹³ Z. Li, G. D. Smith, and D. Bedrov, " Li^+ solvation and transport properties in ionic liquid/lithium salt mixtures: A molecular dynamics simulation study," *J. Phys. Chem. B*, vol. 116, no. 42, pp. 12801–12809, 2012.
- ¹⁹⁴ T. C. Lourenço, Y. Zhang, L. T. Costa, and E. J. Maginn, "A molecular dynamics study of lithium-containing aprotic heterocyclic ionic liquid electrolytes," *J. Chem. Phys.*, vol. 148, no. 19, p. 193834, 2018.

- ¹⁹⁵ M. Z. Bazant, B. D. Storey, and A. A. Kornyshev, "Double layer in ionic liquids: Overscreening versus crowding," *Phys. Rev. Lett.*, vol. 106, no. 4, pp. 046102(1)–046102(4), 2011.
- ¹⁹⁶ V. Gómez-González, A. García-Fuente, A. Vega, J. Carrete, O. Cabeza, L. J. Gallego, and L. M. Varela, "A density functional study of charge transfer at the graphene/ionic liquid interface," *J. Phys. Chem. C*, vol. 122, pp. 15070–15077, 2018.
- ¹⁹⁷ O. Hollóczki, F. Malberg, T. Welton, and B. Kirchner, "On the origin of ionicity in ionic liquids. Ion pairing versus charge transfer," *Physical Chemistry Chemical Physics*, vol. 16, no. 32, pp. 16880–16890, 2014.
- ¹⁹⁸ K. Angenendt and P. Johansson, "Ionic liquid based lithium battery electrolytes: charge carriers and interactions derived by density functional theory calculations," *The J. Phys. Chem. B*, vol. 115, no. 24, pp. 7808–7813, 2011.
- ¹⁹⁹ J. B. Haskins, C. W. Bauschlicher Jr, and J. W. Lawson, "Ab initio simulations and electronic structure of lithium-doped ionic liquids: structure, transport, and electrochemical stability," *The J. Phys. Chem. B*, vol. 119, no. 46, pp. 14705–14719, 2015.
- ²⁰⁰ D. W. Small, D. V. Matyushov, and G. A. Voth, "The theory of electron transfer reactions: what may be missing?," *J. Am. Chem. Soc.*, vol. 125, no. 24, pp. 7470–7478, 2003.
- ²⁰¹ J. Blumberger, " $\text{Cu}_{aq}^+/\text{Cu}_{aq}^{2+}$ redox reaction exhibits strong nonlinear solvent response due to change in coordination number," *J. Am. Chem. Soc.*, vol. 130, no. 47, pp. 16065–16068, 2008.
- ²⁰² H. Yildirim, J. B. Haskins, C. W. Bauschlicher Jr, and J. W. Lawson, "Decomposition of ionic liquids at lithium interfaces. 1. Ab initio molecular dynamics simulations," *J. Phys. Chem. C*, vol. 121, no. 51, pp. 28214–28234, 2017.

- ²⁰³ A. Lozano, B. Escribano, E. Akhmatkaya, and J. Carrasco, "Assessment of van der Waals inclusive density functional theory methods for layered electroactive materials," *Phys. Chem. Chem. Phys.*, vol. 19, no. 15, pp. 10133–10139, 2017.
- ²⁰⁴ K. T. Chan, J. B. Neaton, and M. L. Cohen, "First-principles study of metal adatom adsorption on graphene," *Phys. Rev. B*, vol. 77, pp. 235430–235441, Jun 2008.
- ²⁰⁵ G. Henkelman, A. Arnaldsson, and H. Jónsson, "A fast and robust algorithm for bader decomposition of charge density," *Comp. Mater. Sci.*, vol. 36, no. 3, pp. 354–360, 2006.
- ²⁰⁶ E. Sanville, S. D. Kenny, R. Smith, and G. Henkelman, "Improved grid-based algorithm for Bader charge allocation," *J. Comput. Chem.*, vol. 28, no. 5, pp. 899–908, 2007.
- ²⁰⁷ W. Tang, E. Sanville, and G. Henkelman, "A grid-based Bader analysis algorithm without lattice bias," *J. Phys. Condens. Matter*, vol. 21, no. 8, pp. 084204–084210, 2009.
- ²⁰⁸ M. Yu and D. R. Trinkle, "Accurate and efficient algorithm for Bader charge integration," *J. Chem. Phys.*, vol. 134, no. 6, pp. 064111–064118, 2011.
- ²⁰⁹ F. Aguilera-Granja and L. Gallego, "Structural and electronic properties of $\text{Ni}_{26-p}\text{X}_p$ clusters ($\text{X} = \text{Pd}, \text{Pt}$): a density-functional-theoretic study," *J. Appl. Phys.*, vol. 114, no. 5, pp. 054311–054317, 2013.
- ²¹⁰ F. Aguilera-Granja, J. Carrete, A. Vega, and L. J. Gallego, "Structural, magnetic, and vibrational properties of stoichiometric clusters of CrN ," *Int. J. Quantum Chem.*, vol. 115, no. 8, pp. 523–528, 2015.

List of Tables

2.1	Preferential adsorption, $\Delta\omega(X^{n+})$ ($X^{n+}=\text{Li}^+, \text{Mg}^{2+}$), for mixtures of $[\text{BMIm}][\text{BF}_4]$ with $\text{Mg}[\text{BF}_4]_2$ and, for comparison, with $\text{Li}[\text{BF}_4]$	45
2.2	Coordination numbers, n_{coord} , effective ionic radii, r , surface charge densities, $\sigma = z/4\pi r^2$, and electrostatic field in the ion surface, $U(r_{\text{ion}}) = z/4\pi r$, for various salt cations, X^{+z} , in mixtures with EAN. Radii were taken from Ref. 191. Note that we are using units of $\epsilon = 1$, as we do not know the effective dielectric constant in IL media.	94

List of Figures

1.1	Number of publications per year in the past 20 years related to ILs. Data extracted from Web of Science. . . .	2
1.2	Charged fluids comprise most part of soft matter, and ILs are somehow the paradigm of charged complex fluids, because they share properties with most of them, probably except liquid metals, as can be seen in this schematic figure. . . .	7
1.3	Usual anions that form ILs. Reproduced from http://sigmaaldrich.com	9
1.4	Usual cations that form ILs. Reproduced from http://sigmaaldrich.com	10
1.5	Simulation methods and their characteristic time and length scales.	14
1.6	Selfconsistency scheme for DFT calculations. Reproduced from https://www.vasp.at/vasp-workshop/slides/optelectron.pdf	22
2.1	Number densities, $\rho(z)$, for all simulated [BMIm][BF ₄]-Mg[BF ₄] ₂ mixtures (column 1 corresponds to systems with 10% molar fraction of salt while column 2 corresponds to systems with 25% molar fraction of salt). (a) Negative wall, (b) neutral wall and (c) positive wall. For the sake of clarity, densities for magnesium cation in the left side have been multiplied by 5, while in the right side they have been multiplied by 2.	37

2.2	Distances from the first peak of the density profile relative to the graphene wall for Mg^{2+} cations, for all the molar fractions and wall charges studied in this paper (for comparison, also shown are the results obtained in Ref. 51 for the analogous mixtures of Li^+ cations). Dashed lines are guides to the eye.	38
2.3	Density map of anions (blue, darker), cations (red, lighter) and cations of the added salt (green, light) within a slab close to the graphene surface for the pure $[\text{BMIm}][\text{BF}_4]$ (left column), $[\text{BMIm}][\text{BF}_4]-\text{Li}[\text{BF}_4]$ mixtures (center column) and $[\text{BMIm}][\text{BF}_4]-\text{Mg}[\text{BF}_4]_2$ mixtures (right column). All mixtures represented correspond to a 10% molar fraction of salt. Mixed colors (pink) correspond to the superposition of species in the different layers of the slab, whose width is represented by d	40
2.4	Normalized probability distribution of $ \cos(\theta) $ for the $[\text{BMIm}]^+$ cations in the first layer near negatively charged (a), neutral (b) and positively charged (c) graphene walls for mixtures of $[\text{BMIm}][\text{BF}_4]$ with $\text{Mg}[\text{BF}_4]_2$ and $\text{Li}[\text{BF}_4]$ (left side). In the middle and right sides, this distribution is plotted in a 2D map (including the z distance to the wall) for the systems with 10% (middle) and 25% (right side) $\text{Mg}[\text{BF}_4]_2$ molar fraction.	42
2.5	Mg^{2+} free energy profiles in 10% $[\text{BMIm}][\text{BF}_4]-\text{Mg}[\text{BF}_4]_2$ mixture near the (a) negatively charged (b) neutral and (c) positively charged wall, calculated using the PMF method (blue dots; blue line is a guide to the eye) and the probability method (dashed red line).	44
2.6	Mg^{2+} free energy profiles in 25% $[\text{BMIm}][\text{BF}_4]-\text{Mg}[\text{BF}_4]_2$ mixture near the (a) negatively charged (b) neutral and (c) positively charged wall, calculated using the PMF method (blue dots; blue line is a guide to the eye) and the probability method (dashed red line).	44

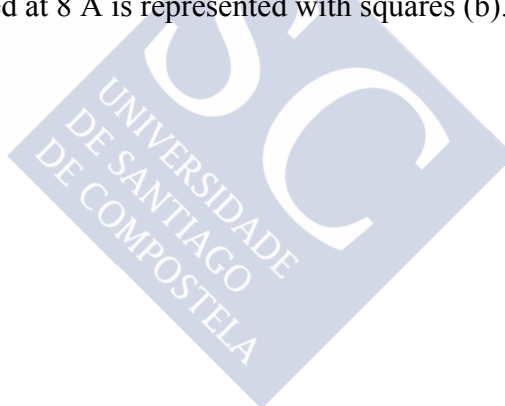
- 2.7 vDOS comparison of Mg^{2+} cation in bulk (shaded in blue) and near the charged walls. (a) 10% molar fraction, (b) 25% molar fraction of salt. 48
- 2.8 Number densities, $\rho(z)$, for all simulated EAN– LiNO_3 mixtures (label 1, above, corresponds to systems with 10% molar fraction of salt while label 2, below, corresponds to systems with 25% molar fraction of salt). (a) Negative wall, (b) neutral wall and (c) positively charged wall. For the sake of clarity, densities for lithium cation in the top figure have been multiplied by 5, while in the bottom figure they have been multiplied by 2. Note that the graphene wall is located at $z = 0$ in all cases. 59
- 2.9 Number densities, $\rho(z)$, for all simulated EAN– $\text{Mg}(\text{NO}_3)_2$ mixtures. All labels have the same meaning as in Fig. 2.8. Note that the graphene wall is located at $z = 0$ in all cases. 60
- 2.10 Normalized continuous probability density functions as a function of $\cos(\theta)$ and the z distance to the wall for the ethylammonium cations in the first layer near negatively charged (a), neutral (b) and positively charged (c) graphene walls for mixtures of EAN with LiNO_3 and $\text{Mg}(\text{NO}_3)_2$. Below, $P(\cos(\theta)) = \int_{zmin}^{zmax} P(z, \cos(\theta)) dz$ is represented. Note that for the sake of clarity the maximum of the color bar above is capped to an optimal value of 2.0 in order to get optimal resolution. 63
- 2.11 Density map of anions (blue, darker), cations (red, lighter) and cations of the added salt (green, light) within the innermost layer closest to the graphene wall for the pure EAN (left column), EAN– LiNO_3 mixtures (center column) and EAN– $\text{Mg}(\text{NO}_3)_2$ mixtures (right column). All mixtures represented correspond to a 10% molar fraction of salt. Mixed colors (pink) correspond to the superposition of species in the different layers of the slab, whose width is represented by d 66

2.12	vDOS comparison of Li^+ cation in bulk (shaded in blue) and near the charged walls. (a) 10% molar fraction of salt, (b) 25% molar fraction of salt.	68
2.13	vDOS comparison of Mg^{2+} cation in bulk (shaded in blue) and near the charged walls. (a) 10% molar fraction of salt, (b) 25% molar fraction of salt.	69
2.14	Distances from the first peak of the density profile relative to the graphene wall for Li^+ and Mg^{2+} cations, for all the molar fractions and wall charges studied in this paper (for comparison, the results obtained in Refs. 51 and 164 for the analogous mixtures of these salts with AILs are also shown). Dashed lines are guides to the eye.	71
2.15	Snapshots of the system of the Li^+ cations closest to the negatively charged graphene wall. C (green), N (blue), O (red), Li (pink) and H (white) atoms are represented. . .	74
2.16	Distances from the wall of a particular lithium atom and its surrounding anions. Faded lines are the values for each simulation step, while solid lines are averaged over the next 100 steps for the sake of clarity. The cation zone is considered to be where the first peak of the cation is placed in the number densities of Fig. 2.8.	75
2.17	Optimized geometries, calculated using DFT, of lithium and its surrounding molecules (7 ionic pairs) without (a) and with a graphene wall (b,c). In (b) the total charge was set to +1e (corresponding to the uncharged interface MD simulation), while in (c) it was set to -3e (negatively charged case).	77
2.18	Comparison of experimental and simulated densities of $\text{Al}(\text{NO}_3)_3$ +EAN mixtures at different salt concentrations.	89
2.19	Experimental, MD and DFT simulated Raman spectrum for the EAN+ $\text{Al}(\text{NO}_3)_3$ mixture.	90
2.20	Salt cation-anion radial distribution functions for different salt cations in their mixtures with EAN. Data for Li taken from Ref. 25 and data for Mg and Ca taken from Ref. 131.	91

2.21	Radial distribution functions of mixtures of EAN with $\text{Al}(\text{NO}_3)_3$. (a) anion–cation, (b) Al–Al, (c) Al–anion, (d) Al–cation.	93
2.22	Total structure factor, $S(q)$, for mixtures of EAN with $\text{Al}(\text{NO}_3)_3$ at different salt concentrations.	95
2.23	Coordination numbers for mixtures of EAN with $\text{Al}(\text{NO}_3)_3$. Dashed lines are guides to the eye. Note that the coordination number of Al–cation corresponds to the second shell of species around salt cations.	96
2.24	DFT optimized structure for a cluster of an aluminium atom and 9 ionic pairs of EAN, including the distances aluminium-anion and aluminium-cation. Note that segments that connect different atoms in the picture are only shown if the distance between those atoms corresponds to their bonding distance.	98
2.25	Hydrogen bonds per molecule in mixtures of EAN with lithium (blue), magnesium (green), calcium (red) and aluminium (orange) nitrates, as well as the predictions of Eq. 2.6, as explained in the text. The black dot corresponds to the value of pure EAN. The inset represents the relative differences between the calculated values and the ideal values of hydrogen bonds, as a function of salt concentration. Data for Li mixtures were taken from Ref. 25, and data for Mg and Ca mixtures were taken from Ref. 131.	100
2.26	Number densities, $\rho(z)$, for all simulated EAN– $\text{Al}(\text{NO}_3)_3$ mixtures (label 1, above, corresponds to systems with 10% molar fraction of salt while label 2, below, corresponds to systems with 25% molar fraction of salt). (a) Negative wall, (b) neutral wall and (c) positively charged wall. For the sake of clarity, densities for aluminium cation in the top figure have been multiplied by 5, while in the bottom figure they have been multiplied by 2.	103

- 2.27 Average minimum distance to the graphene wall of the closest salt cation, for all the molar fractions and wall charges studied in this paper. Monovalent and divalent salt results have been extracted from Ref. 172. Dashed lines are guides to the eye. 106
- 2.28 vDOS comparison of Al^{3+} cation in bulk (shaded in blue) and near the charged walls. (a) 10% molar fraction of salt, (b) 25% molar fraction of salt. 107
- 2.29 Starting configurations for all simulated systems: (a) graphene + Li or Mg cation system, (b) system with fluorine, and (c) system with IL, including the periodic replicas. The dashed red line represents the normal to the graphene surface, along which Li or Mg atoms are moved in order to get the starting geometry of the simulation for each distance to the wall. This line goes through the center of a hexagon of the graphene sheet (hollow site), which is the energetically favored site for the adsorption of group I-III metal adatoms on graphene (see Ref. 204). Atom colors: C, cyan; Li/Mg, pink; F, blue; N, purple; H, white; B, green. 116
- 2.30 Simulated system of $[\text{BMIM}][\text{BF}_4]$ and Li/Mg, and relevant distances between different species. Some replicas of the unit cell (which is shown in Fig. 2.29c) are included for the sake of clarity. The blue arrow represents the direction along which the Li/Mg atom is being moved in order to get the starting geometry of the simulation for each distance to the graphene sheet. 118
- 2.31 Charges of the different species in the system with fluorine as a function of the (a) lithium or (b) magnesium distance to the graphene sheet. The dashed lines represent the charges of salt cation and graphene in the vacuum system. The red dotted line marks the position of the fluorine atom(s). 120

- 2.32 Charges of the different species in the system containing IL as a function of the (a) lithium or (b) magnesium distance to the graphene sheet. Dashed lines represent the charges of salt cation and graphene in the vacuum system. The positions of the other atoms of the system are represented in the background. 121
- 2.33 Relative energies of the simulated systems with Mg, ΔE , as a function of the magnesium distance to the graphene sheet. Note that the origin of energy, $\Delta E = 0$, has been chosen to be that of the configuration with the magnesium atom farthest from the graphene wall. 123
- 2.34 Charges of the different species in the Mg+[BMIM][BF₄] system as a function of the total charge of the system. The system with the Mg atom placed near the graphene sheet (1.6 Å) is represented with dots (a) while the system with this atom placed at 8 Å is represented with squares (b). . 124



List of publications related to this thesis

- **Molecular dynamics simulations of the structure and single-particle dynamics of mixtures of divalent salts and ionic liquids**, Víctor Gómez-González, Borja Docampo-Álvarez, Oscar Cabeza, Maxim Fedorov, Ruth M. Lynden-Bell, Luis J. Gallego, & Luis M. Varela, *J. Chem. Phys.*, **143**(12), 124507 (2015).
- **Molecular dynamics simulation of the structure and interfacial free energy barriers of mixtures of ionic liquids and divalent salts near a graphene wall**, Víctor Gómez-González, Borja Docampo-Álvarez, Trinidad Méndez-Morales, Oscar Cabeza, Vladislav B. Ivaništšev, Maxim V. Fedorov, Luis J. Gallego, & Luis M. Varela, *Phys. Chem. Chem. Phys.*, **19**(1), 846 (2017).
- **Molecular dynamics simulations of the structure of mixtures of protic ionic liquids and monovalent and divalent salts at the electrochemical interface**, Víctor Gómez-González, Borja Docampo-Álvarez, J. Manuel Otero-Mato, Oscar Cabeza, Luis J. Gallego, & Luis M. Varela, *Phys. Chem. Chem. Phys.*, **20**(18), 12767 (2018).
- **Solvation of Al^{3+} cations in bulk and confined protic ionic liquids: a computational study**, Víctor Gómez-González, Borja Docampo-Álvarez, Hadrián Montes-Campos, Juan Carlos Otero, Elena López Lago, Oscar Cabeza, Luis J. Gallego, & Luis M. Varela, *Phys. Chem. Chem. Phys.*, **20** 19071, (2018).
- **A density functional study of charge transfer at the graphene/ionic liquid interface**, Víctor Gómez-González, Amador García-Fuente, Andrés Vega, Jesús Carrete, Oscar Cabeza, Luis J. Gallego, & Luis M. Varela, *J. Phys. Chem. C*, **122** 15070, (2018).

- **Mixtures of protic ionic liquids and molecular cosolvents: A molecular dynamics simulation**, Borja Docampo-Álvarez, Víctor Gómez-González, Trinidad Méndez-Morales, Jesús Carrete, Julio R. Rodríguez, Oscar Cabeza, Luis J. Gallego, & Luis M. Varela, *J. Chem. Phys.*, **140**(21), 214502 (2014).
- **Solvation of molecular cosolvents and inorganic salts in ionic liquids: a review of molecular dynamics simulations**, L.M. Varela, T. Méndez-Morales, J. Carrete, V. Gómez-González, B. Docampo-Álvarez, L.J. Gallego, O. Cabeza, & O. Russina, *J. Mol. Liq.*, **210**, 178 (2015).
- **Structural origin of proton mobility in a protic ionic liquid/imidazole mixture: insights from computational and experimental results**, Negin Yaghini, Víctor Gómez-González, Luis M. Varela, & Anna Martinelli, *Phys. Chem. Chem. Phys.*, **18**(33), 23195 (2016).
- **Molecular dynamics simulations of mixtures of protic and aprotic ionic liquids**, Borja Docampo-Álvarez, Víctor Gómez-González, Trinidad Méndez-Morales, Julio R. Rodríguez, Elena López-Lago, Oscar Cabeza, Luis J. Gallego, & Luis M. Varela, *Phys. Chem. Chem. Phys.*, **18**(34), 23932 (2016).
- **Molecular dynamics simulation of the behaviour of water in nano-confined ionic liquid–water mixtures**, Borja Docampo-Álvarez, Víctor Gómez-González, Hadrián Montes-Campos, José M. Otero-Mato, Trinidad Méndez-Morales, Oscar Cabeza, L.J. Gallego, Ruth M. Lynden-Bell, Vladislav B. Ivaništšev, Maxim V. Fedorov, & Luis M. Varela, *J. Phys. Condens. Matter*, **28**(46), 464001 (2016).
- **Surface and bulk characterisation of mixtures containing alkylammonium nitrates and water or ethanol: Experimental and simulated properties at 298.15 K**, Luisa Segade, Manuel Cabanas, Montserrat Domínguez-Pérez, Esther Rilo, Sandra García-Garabal, Mireille Turmine, Luis M. Varela, Víctor

Gómez-González, Borja Docampo-Alvarez, & Oscar Cabeza, *J. Mol. Liq.*, **222**, 663 (2016).

- **The effect of alkyl chain length on the structure and thermodynamics of protic–aprotic ionic liquid mixtures: a molecular dynamics study**, Borja Docampo-Álvarez, Víctor Gómez-González, Trinidad Méndez-Morales, Julio R. Rodríguez, Oscar Cabeza, Mireille Turmine, Luis J. Gallego, & Luis M. Varela, *Phys. Chem. Chem. Phys.*, **20**(15), 9938 (2018).





